



1 **Characterization of Past Marine Heatwaves around South**
2 **Pacific Island Countries: What really matters?**

3 Shilpa Lal ^{1,2}, Sophie Cravatte ^{1,2}, Christophe Menkes ³, Jed Macdonald ⁴, Romain
4 LeGendre ^{1,3}, Ines Mangolte ³, Cyril Dutheil ⁵, Neil Holbrook ⁶ and Simon Nicol ⁴

5

6 ¹ Université de Toulouse, LEGOS, (IRD/CNES/CNRS/UT3), 31400 Toulouse, France

7 ² Institut de Recherche pour le Développement (IRD) Centre de Nouvelle Calédonie, Nouméa,

8 New Caledonia

9 ³ ENTROPIE, UMR 9220, IRD, Université de la Nouvelle-Calédonie, Université de la Réunion, CNRS,

10 IFREMER, BP 32078, 98897 Nouméa CEDEX, New Caledonia

11 ⁴ Oceanic Fisheries Programme, Fisheries Aquaculture and Marine Ecosystems Division, Pacific Commu-
12 nity (SPC), 98848 Noumea, New Caledonia

13 ⁵ MARBEC, University of Montpellier, CNRS, IFREMER, IRD, Sète, France

14 ⁶ Institute for Marine and Antarctic Studies and ARC Centre of Excellence for Climate Extremes, Univer-
15 sity of Tasmania, Hobart, Tasmania, Australia.

16

17

18

19

20 *Correspondence to:* Shilpa Lal (shilpashupriyalal@gmail.com)

21

22

23



24

25 **Abstract**

26

27 Marine heatwaves (MHWs) can have devastating and lasting impacts on marine ecosystems. We investigated
28 past MHW characteristics around 12 southwestern Pacific Island countries and territories (PICTs) using two
29 observed sea surface temperature products and an ocean reanalysis product. PICTs are highly dependent on
30 their marine resources for their livelihoods: a better understanding of MHW characteristics is needed for
31 planning and adaptation to risks associated with MHWs. Our research builds on previous studies where
32 MHWs have been detected and described using a point-based definition. We first revisit past MHW charac-
33 teristics based on their spatial extent, vertical extent and seasonality. We show that filtering MHWs by size
34 (spatial extent) and seasonality can greatly affect their characterisation and help trace their physical drivers.
35 We then characterise past events inside each EEZ (Economic Exclusive Zone) and at the coast with MHW
36 indices tailored to benefit Pacific Island stakeholders. We consider two types of events: large-scale events,
37 covering a large part of the EEZ, likely to affect pelagic fisheries, and events affecting coastal zones and
38 ecosystems. We distinguish between events occurring in the hot season (November to April), and in the cold
39 season (May to October). We show that all 12 PICTs experienced MHWs in the past 30 years that are getting
40 more frequent with greater spatial extents, longer durations, but with less intensity. New Caledonia, Vanuatu,
41 Fiji and Tonga appear to be more exposed to MHWs with longer duration, higher maximum intensity, and
42 deeper extent compared to other countries.

43

44

45 **1 Introduction**

46 Marine heatwaves (MHWs) are warm ocean temperature extremes, often characterised in terms of anoma-
47 lously warm sea surface temperatures that persist above some threshold value. MHWs have gained traction
48 in recent years by both scientists and the general public due to their detrimental impacts on ecology and the
49 economy. MHWs affect marine life both directly and indirectly, and can reverberate up the food chain. Some
50 iconic events have had devastating effects on coastal species, open-ocean resources and economies at local
51 through to global scales (Hobday et al., 2018; Smith et al., 2021). The 2011 Western Australian event affected
52 several ecological communities including corals, seaweeds, sea grass and commercially important species
53 such as king and tiger prawns, blue crabs and scallops (Caputi et al., 2016; Moore et al., 2012; Thomson et
54 al., 2015; Wernberg et al., 2013). The 2015 northeast Pacific Blob resulted in massive die off in seabirds and
55 mammals, changes in community structure of phytoplankton and zooplankton, and fisheries closures due to
56 harmful algal blooms (Cavole et al., 2016; Jones et al., 2018). The 2012 northwest Atlantic event saw shifts



57 in the distribution and phenological changes in commercially important lobster species, resulting in serious
58 consequences for the lobster fishery in the US and Canada (Mills et al., 2013). Smith et al. (2021) estimate
59 that the economic cost of certain MHW events can exceed several million US dollars (USD) (e.g. \$38 million,
60 2012 northwest Atlantic event) in direct losses and several billion USD per annum in indirect losses for
61 events lasting multiple consecutive years.

62

63 Significant efforts have been made recently to better understand these extreme events, with the ultimate goal
64 to provide useful information to stakeholders to enable effective adaptation measures. As a first step, the need
65 to have a common definition of a MHW, which was valid for both summer and winter seasons and for various
66 areas with different sea surface temperature (SST) variability, was recognised (Hobday et al., 2016, hereafter
67 Hob16). Building on an existing definition developed from the concept of atmospheric heatwave community,
68 Hob16 developed a definition for MHWs. In this now widely used definition, a MHW occurs when ocean
69 (here, sea surface) temperatures are warmer than the daily climatological 90th percentile threshold based on
70 a 30-year historical baseline for a period of five or more days. To better account for the intensity and possible
71 impacts of a MHW, Hobday et al. (2018) further defined MHW categories as integer multiples of the differ-
72 ence between the 90th percentile and the climatological value: these are Moderate (Category 1, between 1 and
73 2 integer multiple), Strong (Category 2, 2-3 integer multiples), Severe (Category 3, 3-4 integer multiples)
74 and Extreme (Category 4, above 4). This definition has been used in many subsequent studies, and statistics
75 obtained on past and future MHWs for the global ocean often rely on this definition, albeit with slight mod-
76 ifications (for example in Oliver et al., 2021; Sen Gupta et al., 2020; Plecha & Soares, 2020). These studies
77 show that all regions in the ocean have been experiencing MHWs in the past decades, with projected increases
78 in MHW intensity, duration and frequency in the coming decades (Oliver et al., 2021).

79

80 Although the southwestern Pacific has been less studied than other regions such as the northeastern Pacific,
81 it has not been spared by MHWs. This region is composed of a myriad of vulnerable islands and atolls, with
82 marine ecosystems and coral reef environments highly sensitive to increasing temperatures, threatening the
83 entire ecosystem and causing concerns for food security, tourism and fish catch rates (Andrefouet et al., 2015;
84 Holbrook et al., 2022; Uthicke et al., 2015; Wyatt et al., 2023, Smith et al., 2021). With the projected increase
85 of temperature, and MHWs frequency with climate change (IPCC, 2023) there are concerns that such eco-
86 systems may disappear completely by 2050 (Dixon et al., 2022; Hughes et al., 2018; van Hooidonk et al.,
87 2013). Holbrook et al. (2022), hereafter H22, examined past MHW characteristics and climate change pro-
88 jections of MHW metrics (frequency, intensity and duration) in the tropical western and central Pacific re-
89 gion. In the whole region (except along the equator), H22 showed that there are on average 1 to 3 MHW
90 events per year at any particular location, typically lasting from 8 to 13 days, with a mean intensity of 1.1°C
91 to 1.7°C. H22 also suggested that MHWs days are projected to significantly increase in the coming decades,
92 with rates depending on the carbon emissions scenario. H22 also investigated 3 main events over the past



93 period: February 2016 event in Fiji, the 2015 mass coral bleaching event in Samoa, and the 2010 mass coral
94 bleaching event in Palau.

95

96 These analyses are a useful first step for Pacific Island countries towards becoming aware of the past and
97 future risk of exposure to MHWs of varying intensities, frequencies and durations. Yet, the information that
98 decision makers could extract from these metrics is often insufficient to allow them to fully understand MHW
99 impacts on ecosystems, and to take effective action. We illustrate this through the following four points. First,
100 as Hob16's detection method is performed independently at each location, it does not consider MHW spatial
101 extent and does not distinguish between large events and smaller, more localised events. Secondly, in most
102 studies, the detection is done at the surface, and does not consider the MHW vertical extent. These metrics
103 alone do not fully measure all ecosystem exposure. Highly mobile pelagic species, such as tunas, are likely
104 not affected in the same way by very localised events that sessile species are. The extent of exposure for
105 mobile species is likely more linked to large-scale events covering hundreds or thousands of square kilome-
106 tres. Many pelagic species also regularly move vertically through the water column to track prey resources
107 and/or meet oxygen demands (Briand et al. 2011; Arrizabalaga et al. 2015; Nikolic et al. 2017), and metrics
108 measuring the depth of MHWs are needed to capture this exposure. Thirdly, seasonal distinctions are essen-
109 tial as MHWs' impacts on ecosystems depend on their thermal tolerance levels, thus on the time of year of
110 occurrence (summer or winter). Finally, time-mean statistics for MHWs alone do not inform decision makers
111 on the strongest events that occurred in the past, nor on the statistical distributions of events, to better antic-
112 ipate the types of future events that are likely to occur in the countries' waters.

113

114 Here, we aim to go beyond these limitations. We characterise past MHWs (1993-2023) for 12 Pacific Island
115 countries and territories (PICTs) within their EEZs, so that the results can be more easily usable for marine
116 management and decision making in each PICT. We consider two different types of events that can signifi-
117 cantly affect Pacific Island ecosystems and economies: (i) large-scale events, henceforth referred to as 'Mac-
118 roscale events', covering a large part of the EEZ, with potentially significant impacts for pelagic fisheries,
119 and (ii) coastal events, that may have smaller spatial extents, yet may impart significant impacts on reef
120 ecosystems and coastal resource management. We distinguish between events occurring in summer and in
121 winter months. We extract the vertical extents of surface MHWs to gain an understanding of the volume of
122 water that may be subjected to heat stress during MHW events. Finally, we also explore climate trends in
123 MHW properties.

124

125 This paper is organised as follows. In section 2, we present the data used, and the methodology applied. In
126 the same vein as some recent studies (Sun et al., 2023; Bonino et al., 2023), we propose an easy and simple
127 way to quantify the spatial extent of surface MHWs by calculating areas of connected points. In section 3,
128 we explore the spatial extent of MHWs in the whole southwest Pacific region, and show that the MHW



129 metrics, when excluding small scale events, change substantially from what has been previously published
130 (H22; Oliver et al., 2021). We also show that discussing MHW statistics in terms of sizes helps to infer the
131 underlying physical drivers. In section 4, we provide information on past MHW characteristics for PICTs.
132 For each PICT, we provide past MHW metrics for the two types of events (macroscale and coastal events),
133 separately. We conclude and provide perspectives in section 5 on what should now be done, with this infor-
134 mation, to better assess the vulnerability of PICTs to future MHWs.

135

136 **2 Data and Methods**

137 The study region extends from 2.4°S to 34.8°S and 145°E to 151°W (Fig. 1 a). It contains the eastern coastline
138 of Australia and Papua New Guinea and full EEZs of 12 PICTs; on the western side, Solomon Islands, New
139 Caledonia, Vanuatu; in the centre, Tuvalu, Fiji, Wallis and Futuna, Tonga; and on the eastern side, Tokelau,
140 Samoa, American Samoa, Niue and Cook Islands.

141

142 **2.1 Temperature datasets**

143 We used three ocean temperature products to detect MHWs over the study region. We first used the NOAA-
144 OISST version 2.1, which is a blended daily SST product (representing temperatures at 0.2m depth) mixing
145 satellite and in situ SST data. These data are mapped onto a 0.25° grid for the period 1981-09-01 to 2023-06-
146 26 (Huang et al., 2021).

147

148 We also used ocean temperatures from GLORYS12, an ocean reanalysis product with a 1/12° horizontal
149 resolution and 50 vertical levels (Lellouche et al., 2021). For comparison with NOAA-OISST, the GLO-
150 RYS12 data was regridded to 0.25° and the first depth level was used (0.49m) for the period 1993-01-01 to
151 2019-12-31 for open ocean events. The advantage of GLORYS12 is that it allows us to explore the vertical
152 extent of MHWs. For investigation of the MHW events at the coast (Section 4), grid cells closest to the land
153 mask of the 12 PICTs in waters deeper than 200m depth were used at 1/12° horizontal resolution and at the
154 first depth level (0.49m) for the period 1993-01-01 to 2023-10-24. As GLORYS12 does not resolve processes
155 in very shallow coastal waters adequately, a depth of 200m allowed MHW detection to be made in suffi-
156 ciently deep waters outside the lagoon but close enough to the coast so that inferences could be made about
157 MHW events that could have affected coastal waters.

158



159 Finally, we use the Operational Sea Surface Temperature and Ice Analysis (OSTIA) product to validate and
160 compare robust features in coastal MHWs with GLORYS12. OSTIA is a 0.05° horizontal resolution, blended
161 SST product using in-situ and satellite data from both infrared and microwave radiometers (Good et al.,
162 2020).

163

164 **2.2 MHW detection method and product intercomparison**

165 MHWs were detected using all products, based on the Hob16 definition at each pixel in the tropical southwest
166 Pacific (Fig. 1 a). A 90th percentile threshold was used with the 1993-2019 climatological period. This base-
167 line was chosen since it was common to all products and for consistency, as the detection method is quite
168 sensitive to the baseline chosen (Amaya et al., 2023). No trend was removed. The marineHeatWaves package
169 available in Python (<https://github.com/ecjoliver/marineHeatWaves>, last access: 24 September 2024) was
170 used for the detection of MHWs and calculation of key MHW parameters such as duration, intensities, onset
171 and decline rates.

172

173 We also computed linear trends for the annual number of MHW days, duration, max intensity, vertical extent
174 and their significance using linear least-squares regression from the Scipy Package in Python. For the detec-
175 tion and calculation of trends, annual mean time series of these variables were used for full years from 1982
176 to 2022 for NOAA-OISST and 1993 to 2022 for GLORYS12 and OSTIA coastal events.

177 The statistical significance of the slope was obtained with the parametric Wald Test ([https:// docs.scipy.org
178 /doc/scipy/reference/generated/ scipy.stats.linregress.htm](https://docs.scipy.org/doc/scipy/reference/generated/scipy.stats.linregress.htm), last access: 6 July 2024).

179

180 **2.3 MHW spatial extent**

181 Here we present a simple and easy way to measure the daily spatial extent of MHWs, using contours drawn
182 over spatially connected MHW patches. It is an intuitive method, easy to follow and sufficient for the pur-
183 poses of this paper, allowing MHWs to be described in a way complementary to the parameters originally
184 presented in Hob16. As in the method used by Bonino et al. (2023), our method does not consider the physical
185 processes behind an event, it just calculates the area occupied by connected pixels in active MHW state.

186

187 After MHWs were detected at each grid cell in the study area (Fig. 1 a), a boolean 1 was assigned to each
188 day in an active MHW state at each location and a 0 otherwise. Contours were drawn over regions with 1s
189 and 0s. The closed contours were then turned into polygons and the area of the polygons were calculated. In
190 the case where non-MHW areas were enclosed by MHW areas, the area occupied by the non-MHW polygon
191 was subtracted from the MHW polygon. Each grid cell within a particular MHW polygon was assigned a



192 value equal to the area of that MHW polygon (Fig. 1 b). Polygons greater than 25 square degrees were cate-
193 gorised as ‘macroscale’ events and polygons smaller than 25 square degrees as ‘microscale’ events on each
194 day. This choice follows Sun et al. (2023) and allows the elimination of the MHWs linked to the passage of
195 mesoscale eddies, which occupy areas of around 1-2 square degrees, with diameters between 50-500 km in
196 the region (Keppler et al., 2018). The micro and macroscale spatial extents were then associated to the time
197 series of MHW properties described in Section 2.2 (MHW detection method and product intercomparison)
198 to filter the events by their spatial extent. Once information relevant to events of particular spatial extent were
199 obtained, comparisons between the MHW properties related to microscale and macroscale events were made
200 by sizes and seasons. Properties associated with macroscale events were then clipped with country EEZs to
201 obtain relevant country level information.

202

203 **2.4 MHW vertical extent**

204 MHWs were identified independently at each of the upper ocean 38 depth levels available in GLORYS12
205 from 0.49 to 1500m, as has been done by others (Schaeffer et al., 2023; Schaeffer & Roughan, 2017). We
206 only consider events detected at the surface. Then, the maximum depth of MHW detection without interrup-
207 tion from the surface in MHW detection, was recorded as the vertical extent of the surface MHW event at
208 that location. This method does not allow for the identification of subsurface-only MHWs (Schaeffer et al.,
209 2023). Vertical extents associated with microscale and macroscale events were explored in terms of their
210 seasonality and trends. Macroscale events were clipped with country EEZs to obtain relevant country level
211 information.

212



213

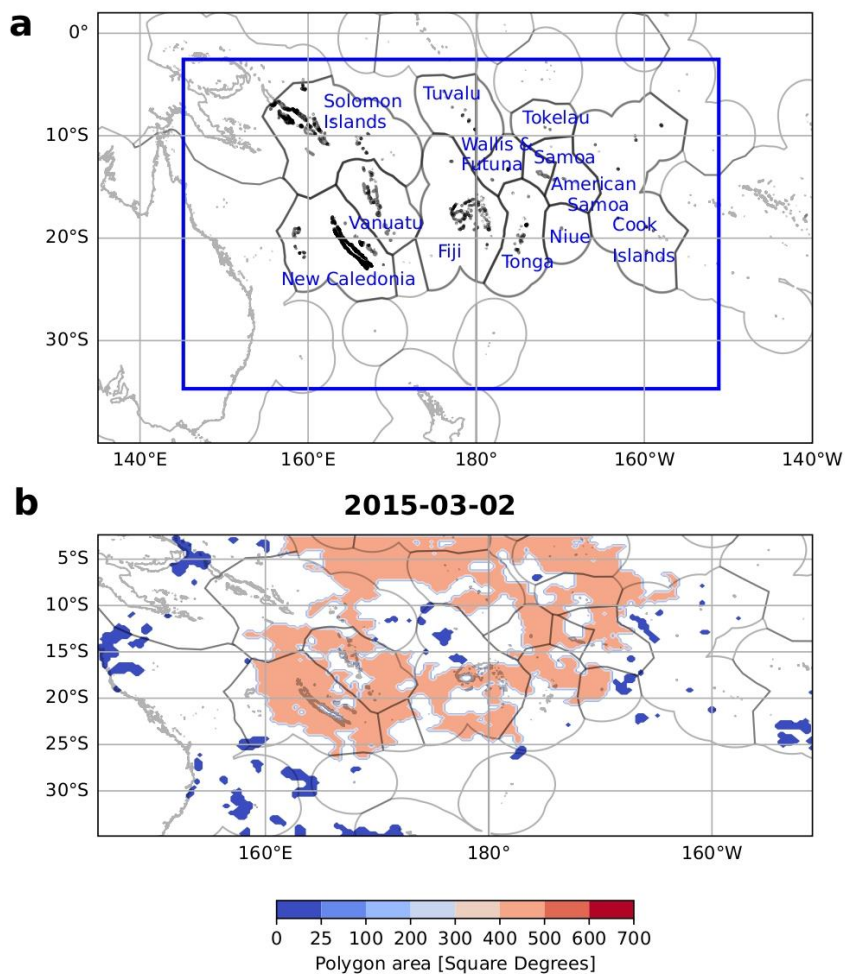


Figure 1 a. Map showing the study area, tropical South Western Pacific enclosed by the blue box. The 12 PICTs explored in depth in this study with their Exclusive Economic Zones (EEZs) are labelled in blue and outlined in black inside the blue box, from left to right Solomon Islands, New Caledonia, Vanuatu, Tuvalu, Fiji, Wallis and Futuna, Tonga, Tokelau, Samoa, American Samoa, Niue and Cook Islands. Other PICTs and their EEZs in the region are outlined in grey. b. MHW polygon areas on 2015-03-02. MHWs detected using NOAA-OISST from 1981-09 to 2023-06.



214 **3 Revisiting past MHW metrics in the southwest Pacific in terms of spatial extent and seasonality**

215 **3.1 MHW spatial extent**

216 Before characterising “macroscale” MHW events, we first investigate the distribution of MHW polygon sizes
217 in the study region. Figure 2 shows histograms of MHW polygons, by size, for both NOAA-OISST and
218 GLORYS12 products, and separately for cold season (May to October) and hot season (November to April).
219 A large majority of the MHW events (80% for GLORYS12, 72% for NOAA-OISST) detected daily are of
220 very small spatial extent, less than one square degree (Fig. 2 a). The two products give quite different results
221 for the number of small-scale events, highlighting the dependence of the Hob16 detection method on the
222 product used. Hob16 have acknowledged that the method is sensitive to the product chosen, and differences
223 may arise in terms of MHWs statistics among products, even when using the same baseline (see Appendix
224 1). This is particularly true in the cold season, when there are more than twice as many events smaller than 1
225 square degree identified using GLORYS12 compared with the NOAA-OISST product (Fig. 2 a). This might
226 also be related to higher energy of fine-scale processes in the cold season in the region (Rocha et al., 2016;
227 Sérazin et al., 2019) represented in the 1/12° GLORYS simulation. Interestingly, the differences in the
228 number of macroscale polygons (i.e. polygons greater than 25 square degrees) between the two products is
229 strongly reduced (17% difference between NOAA-OISST and GLORYS12 compared to 94% difference for
230 sizes smaller than 25 square degrees, not shown). This is an important result, since it lowers the dependence
231 of the method on the product used when examining properties of macroscale events. Up to 20 square degrees,
232 microscale events are more numerous in the cold season than in the hot season (18% and 60% more, for
233 NOAA-OISST and GLORYS12, respectively, Fig. 2 b). The contrary is true for macroscale events: there are
234 more macroscale events in the hot season than in the cold season (37% and 32% more, for NOAA-OISST
235 and GLORYS12, respectively, Fig. 2 b) as will be discussed later.

236

237

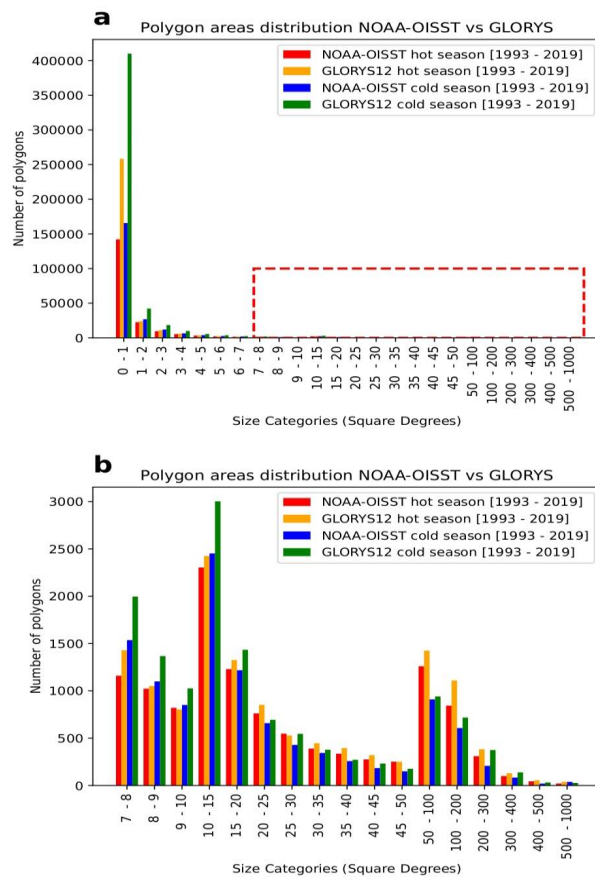


Figure 2 Bar chart showing the number of MHW polygons belonging to various size categories in the hot (November to April) and cold (May to October) seasons. a, Shows all the size categories from 0 to 1000 square degrees. The red dashed rectangle is to indicate the zoom used in b. b, is a zoom in on sizes 7 to 1000 square degrees. Polygon areas were calculated from MHWs detected using NOAA-OISST and GLORYS12 from years 1993 to 2019.



239 Figure 3 shows the median size of the MHWs occurring in the southwest Pacific region. MHWs have highly
240 variable spatial extents throughout the region. The majority of events occurring around New Caledonia, Va-
241 nuatu and Fiji are large-scale events of more than 160 square degrees (Fig. 3). This suggests that for these
242 areas, the underlying processes could be linked to drivers impacting large-scale atmospheric or oceanic condi-
243 tions, such as ENSO or MJO (Madden Julian Oscillation), as suggested previously (Dutheil et al., 2024;
244 Holbrook et al., 2019; Sen Gupta et al., 2020; Vogt et al., 2022). MHWs become slightly smaller towards the
245 east, with a median size of less than 100 square degrees. In the eddy-rich region associated with the East
246 Australian Current and its retroflexion (west of $\sim 170^\circ\text{E}$ and south of 25°S), MHWs are all small sized, with
247 the median being smaller than the 25 square degrees limit (marked in dashed lines in magenta, Fig. 3). They
248 are mostly associated with the occurrence of mesoscale eddies. MHWs are also small in the Warm Pool
249 region, equatorward of 5°S (Fig. 3).

250

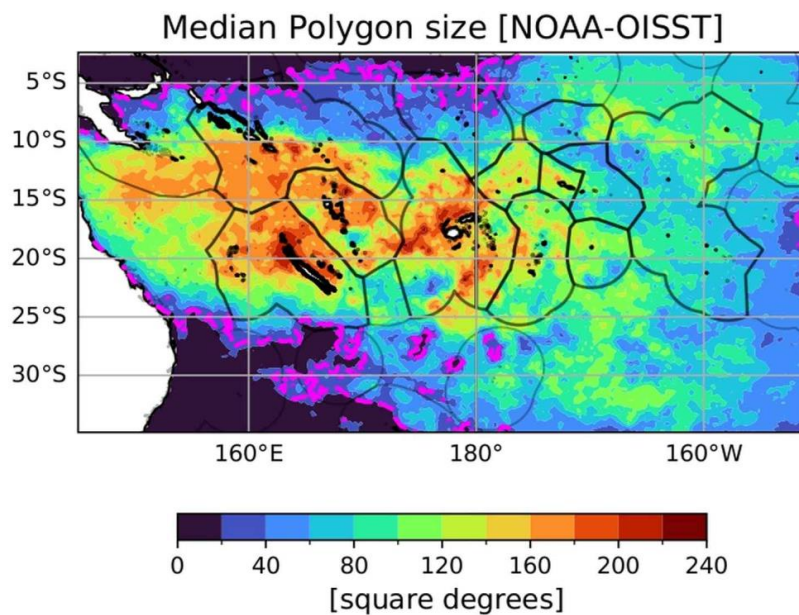


Figure 3 Map showing median MHW polygon size with a dashed contour line at 25 square degrees in magenta. MHWs detected using NOAA-OISST from 1981-09 to 2023-06.

251



252 **3.2 Properties of MHWs filtered by size and season**

253 Investigating the properties of MHWs (number of MHW days, mean duration, mean maximum intensity and
254 vertical extent) as a function of size and season revealed patterns resembling dominant ocean-atmosphere
255 processes in regions within the study area. The climate of the region is largely influenced by the presence of
256 the South Pacific Convergence Zone (SPCZ), a band of low-level atmospheric convergence, cloudiness and
257 rainfall, roughly extending from the Solomon Islands southeastward toward French Polynesia (Brown et al.
258 2020; Vincent et al., 2014). In the northern part of the region, equatorward of $\sim 10^{\circ}\text{S}$, the waters are warmer
259 than 29°C , forming the western Pacific Warm Pool (Cravatte et al., 2009). The region south of 20°S , in the
260 area of the Subtropical CounterCurrent and in the area of the meandering East Australian Current, is charac-
261 terized by ubiquitous, long lived, deep extending mesoscale eddies (Keppler et al., 2018; Qiu et al., 2009).
262 We chose to divide the study area into five subregions based on common MHW characteristics occurring in
263 these regions; 1. South-SPCZ region, 2. North-SPCZ region, 3. Equatorial central region, 4. Southeastern
264 Australia eddy region and 5. Subtropical region. Fig. 4 shows mean MHW characteristics for all events, and
265 also separately for microscale (0-25 square degrees) and macroscale events (25-700 square degrees). Figure
266 5 further shows these properties for the hot and cold seasons for macroscale events. Figure 6 shows the mean
267 vertical extent of the MHWs for both micro and macroscale events for the two seasons.

268
269 Across the whole study area, there are between 10 to 30 days of MHWs per year (Fig. 4 a), with contrasting
270 properties within the domain. Subregion 2 stands out with less MHW days than the rest of the region (around
271 12 to 18 days per year), with a similar amount of microscale and macroscale events all year around, i.e., in
272 both the cold season and hot season (Fig. 5 for macroscale only, microscale not shown). There, MHWs are
273 of short duration (typically 5 to 10 days), and of small maximum intensities ($+1.4^{\circ}\text{C}$). This subregion corre-
274 sponds to the location of the warmest surface waters of the Warm Pool, where temperatures are greater than
275 29°C in the mean (blue contour in Fig. 4 a), and where the cloud cover is important. MHWs here extend from
276 40 to 80m depth in the hot season, deeper than the mean mixed layer depth, and even deeper in colder months
277 (Fig. 6).

278
279 In contrast, subregion 3 (the equatorial region east of 180° central region) is exposed to MHWs around 25 to
280 30 days per year (Fig. 4 a). There, the majority of MHWs are large-scale events (compare Fig. 4 d and g) and
281 most present during the hot months (Fig. 5). These MHWs are of longer duration (on average 40 days) and
282 of higher intensities (approx. $+2^{\circ}\text{C}$) closer to the equatorial band and they extend quite deeply (down to 80
283 to 100 m depth, Fig. 6 c, d). These long duration, large-scale and deep MHWs are systematically associated
284 with El Nino events (not shown), and consistent with processes associated with the eastward displacement
285 of the Warm Pool waters and deepening of the thermocline in the region during the development of El Nino
286 events (e.g. Picaut et al. 2001).



287

288 Subregion 1, the “South-SPCZ region” is, interestingly, the region which is more exposed to MHWs, with as
289 much as 30 days of MHWs per year on average. This area encompasses the Solomon Sea and the Coral Sea,
290 and extends eastward to the Fiji archipelago. There, the MHWs are mostly of large scale (compare Fig. 4 d
291 and g, see also Fig. 3), and associated with long durations (more than 30 days on average, Fig. 4 h). Their
292 maximum intensity is slightly greater for macroscale events than microscale, typically being around +1.6 to
293 +2°C. In the hot season, macroscale events are more numerous but of shorter duration compared to the cold
294 season. Their depth corresponds to the mean seasonal depth of the mixed layer, typically from 20 to 40m in
295 the hot season and from 40 to 80m in the cold season (Fig. 6). In the cold season, macroscale events are less
296 numerous, but last longer: some can last up to one year (see Fig. 5 e). They are slightly deeper, typically from
297 40 to 80m, also mirroring the winter depth of the mixed layer (Fig. 6). The very long events in the cold season
298 correspond to the recent La Niña years, as will be discussed later, and to the associated warmer anomalous
299 SST conditions in the southwest Pacific. More studies will be required to characterise the processes driving
300 other MHW events, but the characteristics described here argue for mixed layer dynamics and large-scale
301 atmospheric forcing events.

302

303 Subregion 4, the “Southeastern Australia eddy region”, is characterised by 15 to 25 MHW days per year. In
304 this eddy-rich area, associated with the retroflection of the energetic East Australian Current, MHWs events
305 are all of small size and short duration (10 to 25 days). They have large maximum intensities, reaching above
306 3.5°C south of the domain. These microscale MHWs exhibit substantial vertical extent, much deeper than
307 the mixed layer depth, both in the hot season (100 to 150m) and in the cold season (more than 200m) sug-
308 gesting that they are mostly associated with passing eddies (see Fig. 6) with deeper impacts in winter (Bian
309 et al., 2023).

310

311 Finally, subregion 5, the “subtropical region”, is a mix between subregions 1 and 4 in terms of MHW prop-
312 erties. This area experiences between 20 and 32 days of MHWs each year (Fig. 4 a), both of large and small
313 scales. As with subregion 1, the macroscale events are more prevalent in the hot season (Fig. 5 a), with short
314 durations of 10 to 20 days, but large intensities (2 to 2.5°C), and shallow depths (20 to 40 m depth, corre-
315 sponding to the mean seasonal depth of the mixed layer, see Fig. 6). Very few macroscale events occur in the
316 cold season, but they do last longer than in summer and are on average of lower intensity (+1.4 to +2°C). It
317 is worth noting that MHW properties are quite noisy here, with small-scale features of longer duration, higher
318 intensities, and overall much deeper extent (Fig. 6). It is probable that these MHWs arise through several
319 processes, with large-scale atmospheric forcing contributing to large-scale, shallow events, and mesoscale
320 eddies contributing to smaller scale events, with much deeper extents, as also suggested by Bian et al. (2023).

321



322 Overall, seasonality appears to play a very important role in the characterisation of MHW properties in the
 323 study region. For macroscale events, MHW properties have contrasting characteristics in different seasons.
 324 This suggests that the combination of drivers of MHW events in the hot and cold seasons may actually be
 325 quite different. In general, over the study area, there is a tendency for macroscale events to be of short dura-
 326 tion and high maximum intensity during the hot season, while the opposite is true for the cold season. While
 327 microscale events tend to have higher variability in terms of vertical extent, and can extend deeper than
 328 macroscale events in some locations regardless of the season (compare Fig. 6 a, b to c, d), both microscale
 329 events and macroscale events are much shallower in the hot season and extend much deeper in the cold
 330 season. This is likely due to shoaling of the mixed layer depth (MLD) during the hot season (median MLD
 331 ~14-28m, Fig. 6 e), restricting surface related MHWs within the shallower mixed layer, and due to deeper
 332 MLD in the cold season (median MLD ~14-90m, Fig. 6 f) allowing greater mixing and MHWs to be detected
 333 without interruption over greater depths.

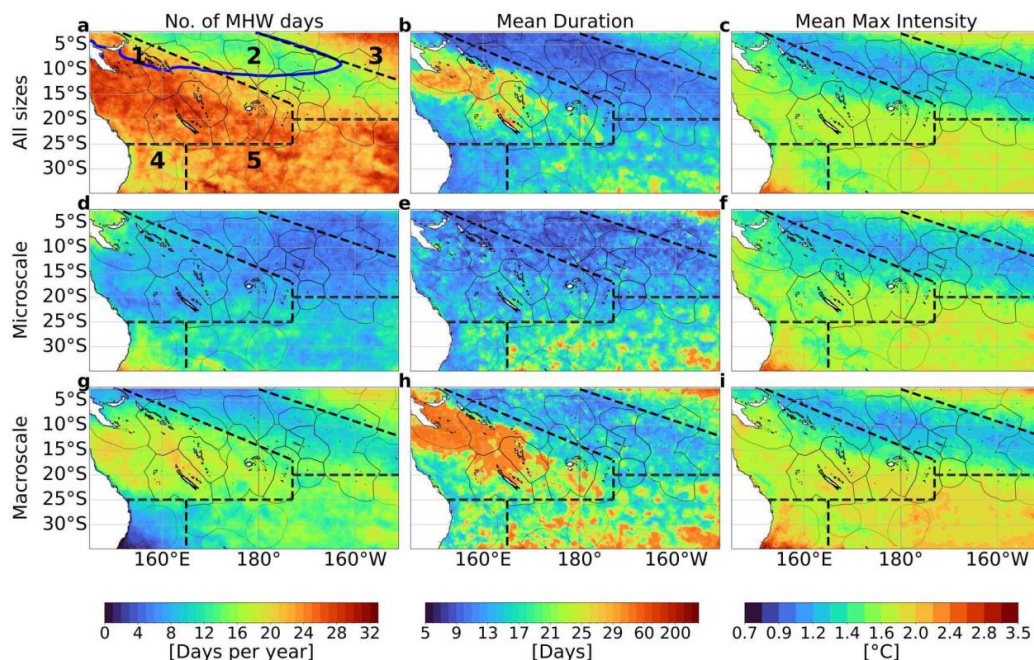


Figure 4 Panel plots showing number of MHW days, mean duration and max intensity by spatial extent; a,b,c, for all sizes (0-700 square degrees), d,e,f, for microscale (sizes 0-25 square degrees), g,h,i for macroscale (sizes 25-700 square degrees) respectively. MHWs detected using NOAA-OISST from 1981-09 to 2023-06. Regions of special interest based on common ocean-atmospheric process demarcated with black dashed lines; 1. South-SPCZ region, 2. North-SPCZ region, 3. Equatorial central region, 4. Southeastern Australia eddy region and 5. Subtropical region. The blue line in a is the 29°C isotherm (mean temperature) showing the mean position of the western Pacific warm pool.



335

336

337

338

339

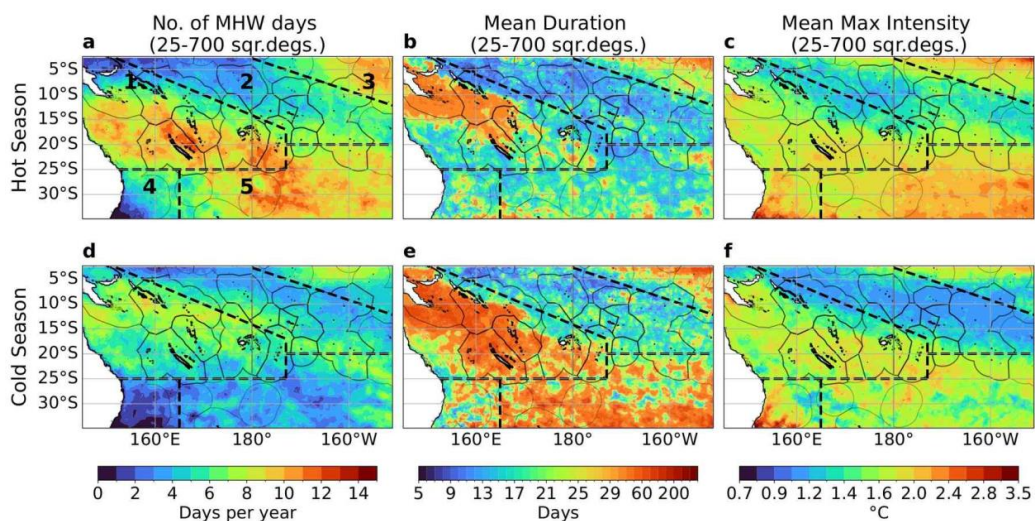


Figure 5 Panel plots showing number of MHW days, mean duration and mean max intensity for macroscale events (25-700 square degrees); a,b,c in hot and d,e,f in cold season respectively. MHWs detected using NOAA-OISST from 1981-09 to 2023-06. Refer to Figure 4a for regions numbered 1 - 5, demarcated with black dashed lines.

340

341

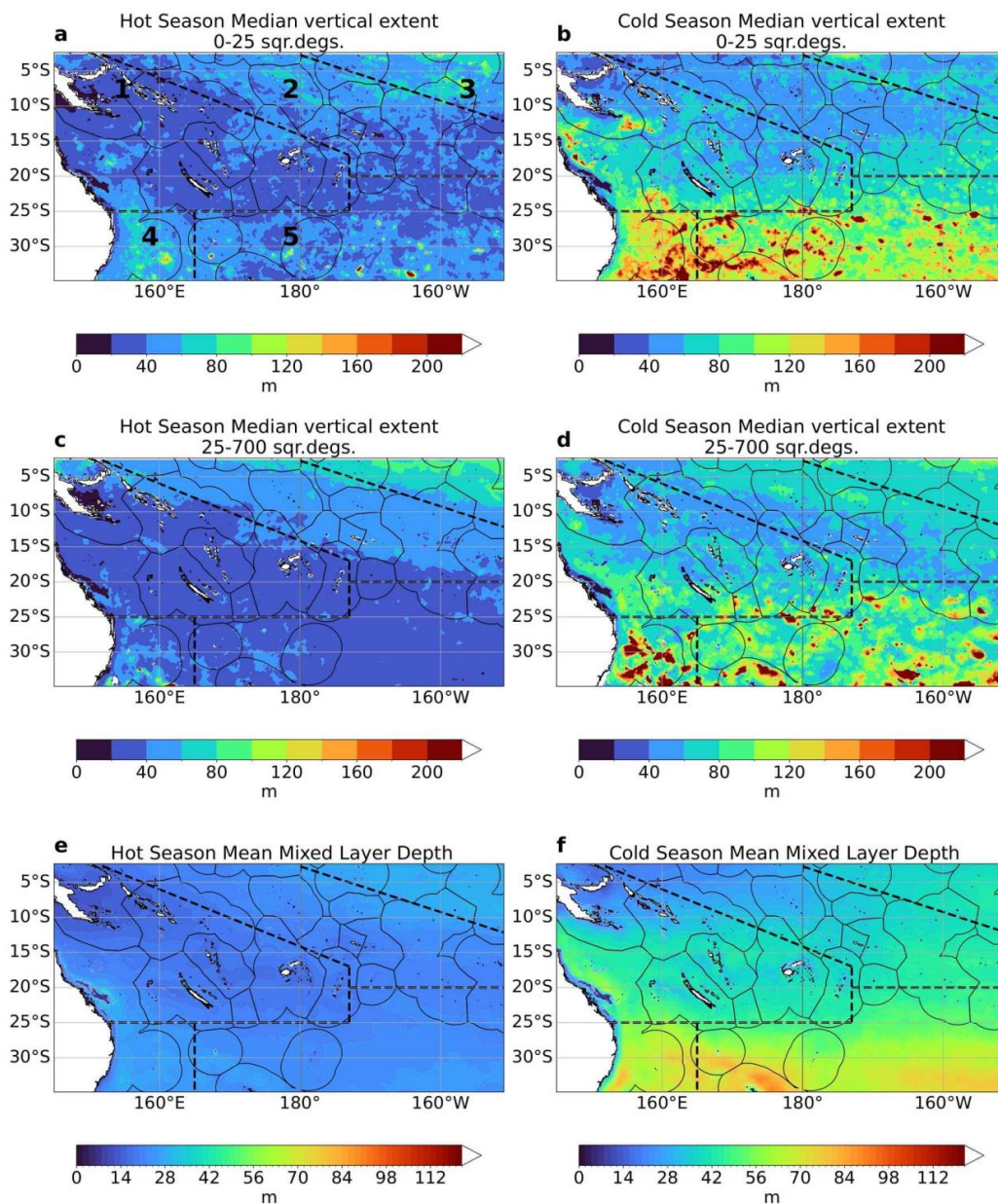


Figure 6 Median vertical extent of surface MHWs by spatial extent and seasons; a,b, microscale events (0-25 square degrees) in hot and cold seasons respectively. c,d, macroscale events (25-700 square degrees) in hot and cold seasons respectively. e,f, Mean mixed layer depth in hot and cold seasons respectively from GLORYS12. MHWs detected using GLORYS12 from 1993 to 2019. Refer to Figure 4a for regions numbered 1 - 5, demarcated with black dashed lines.



343 **3.3 Long term trends**

344 The previous figures showed the mean MHW properties over the 1981-2023 period. A key question now is
345 whether if, and how, these properties have changed over time. This was investigated in H22. They found that,
346 except for the central equatorial subregion 3, there has been an increase in the number of events per year, but
347 with no strong nor consistent trend in intensity or duration. Here, we focus on the macroscale events. Figure
348 7 shows trends in annual number of MHW days, duration, max intensity and vertical extent, with hatched
349 areas indicating significant (p -value < 0.05) trends for macroscale events. For subregions 1, 2 and 5, the
350 number of MHWs per year significantly increased over time. As the 12 countries studied in detail are located
351 in these three regions, all countries also have significant positive trends in the annual number of MHW days
352 (Fig. 7 a). Region 1 experiences between 12 to 24 MHW days per year on average (Fig. 4 g); this number
353 doubled per decade around the Solomon Islands, New Caledonia and Vanuatu (Fig. 7 a). The same is true for
354 the trend in MHW duration, with MHW events becoming longer over the past decades (Fig. 7 b). Average
355 MHW duration is between 5 – 30 days over most of the countries (Fig. 4). The mean duration has doubled
356 per decade, since 1982, especially in subregion 1, in the Solomon Sea. On the contrary, and consistent with
357 H22 findings, there is no strong and significant trend in MHW intensity (Fig. 7 c). The only significant pattern
358 is a decreased intensity in the Warm Pool area (subregion 2), where the intensity was already the smallest in
359 the whole region. No significant trends were observed over most parts of the study region in terms of the
360 vertical extent (Fig. 7 d). Finally, Fig. 8 shows the daily time series of the percentage of surface area of the
361 study region in a MHW state, for both GLORYS12 and NOAA-OISST. A significant trend of ~3.5 percent
362 (~70 square degrees) increase per decade is observed (Fig. 8). Over the past decade, there has not been a
363 single day when at least part of the region was not exposed to a MHW.

364
365
366
367
368
369
370
371
372
373
374
375
376
377



378

379

380

381

382

383

384

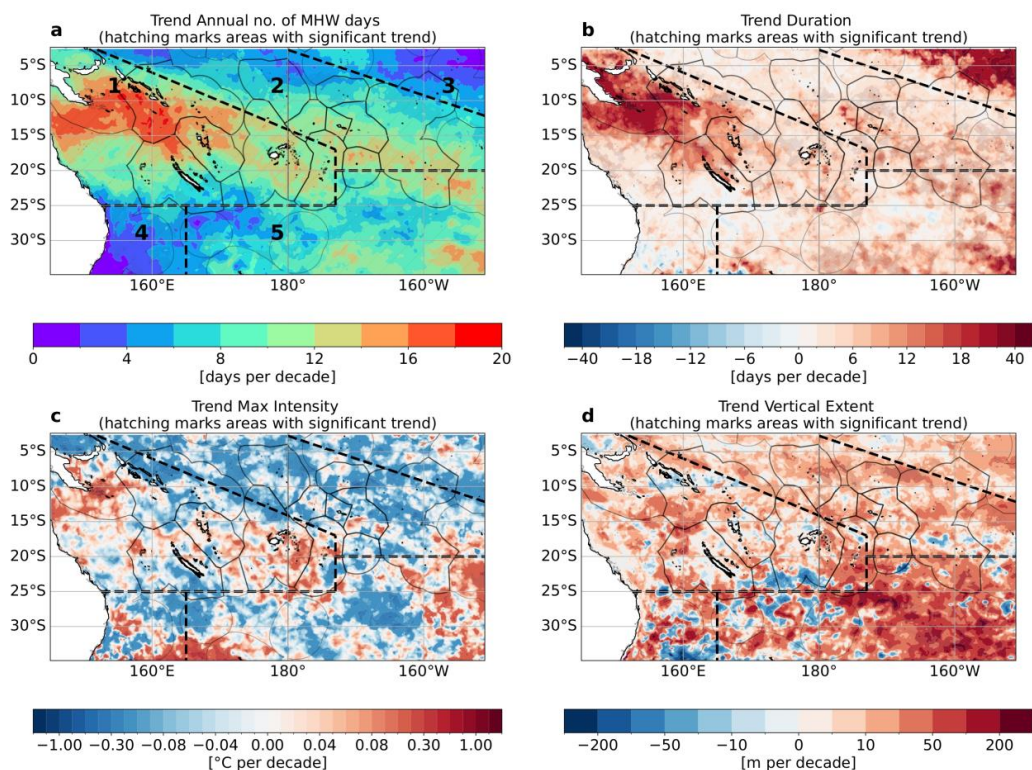


Figure 7 Trends in a, annual number of MHW days, b, duration, c, maximum intensity and d, vertical extent associated with macroscale events. MHWs detected using NOAA-OISST from 1982 to 2022. The regions demarcated in black are, 1. South-SPCZ region, 2. North-SPCZ region, 3. Equatorial central region, 4. Southeastern Australia eddy region and 5. Subtropical region. The data in the maps refer to average changes in these metrics per decade over the 40 years.

385



386

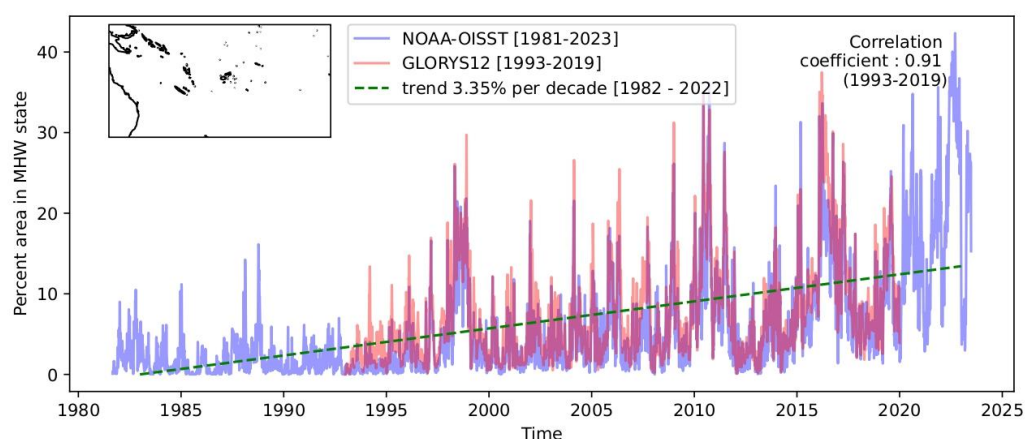


Figure 8 Timeseries showing percent of study region in MHW state, with a statistically significant trend line (p -value < 0.05) in green calculated between 1982 to 2022 for NOAA-OISST and Pearson correlation coefficient calculated between 1993 and 2019 for NOAA-OISST and GLORYS12 (p -value < 0.05).

387

388 **4 Past MHWs for each Pacific country**

389 **4.1 Macroscale events: statistics for each country**

390 Section 3 discussed MHW properties at the regional scale. To provide more usable information for PICTs,
391 we now investigate statistics of past macroscale events that affected each EEZ separately. Figure 9 shows the
392 mean and standard deviation of the mean duration and mean max intensity in the 12 PICTs studied. PICTs
393 in the western and south-central part of the study region: Solomon Islands, New Caledonia, Vanuatu, Fiji and
394 Tonga appear to be more exposed to MHWs of higher duration (Fig. 9 a) but with a large variability in MHW
395 duration (Fig. 9 b). These PICTs are also exposed to higher maximum intensity events (Fig. 9 c) with a
396 higher standard deviation (Fig. 3.9d) compared to other PICTs (Fig. 9), suggesting that the types of MHWs
397 to which they are exposed are more diverse in terms of features and possible drivers. Figure 10 illustrates the
398 seasonal distribution of macroscale MHW properties (i.e. MHW duration, maximum intensity, onset rate,
399 decline rate and vertical extent) inside the EEZs of each of the 12 PICTs. These properties have been chosen
400 for their relevance for marine ecosystem management and to help guide adaptation planning across the Pa-
401 cific region. Maximum intensity and onset and decline rates (two MHW metrics describing how quickly a



402 MHW develops or dissipates) are of particular interest (Jessica Randall per. communication) as these param-
403 eters allow managers to gauge the amount of time they would need to better prepare for MHWs, and the
404 potential severity of their impacts (Spillman et al., 2021; Jessica Randall per. communication).

405 Figure 10 confirms, at EEZ scales, and similar to the results presented in section 3, that in the hot season,
406 most of the macroscale events in all countries are of short duration. Half of the MHW events lasted < 10
407 days, 75% of the events were < 20 days (Fig. 10a), and for most of the PICTs, 90% of the MHWs lasted <
408 30 days. However, there is some variability among the PICTs; 90% of the MHWs events affecting Tuvalu
409 were < 20 days, whereas 10% of the events affecting Vanuatu were > 50 days. (Fig. 10 a). In the cold season,
410 the MHW duration is more variable, and events can last much longer. This is especially true for PICTs within
411 subregion 1 (New Caledonia, and Vanuatu) which experienced 25% of events > 40 days and 10% of the
412 events lasting up to 4 to 5 months (Fig. 10 a). New Caledonia and Vanuatu also experienced the highest
413 maximum intensities compared to other PICTs, followed by Tonga and Fiji.

414

415 For PICTs located in the eastern part of the region, the median maximum intensities are between 0.25 to
416 0.5°C higher in the hot season than in the cold season, for example in American Samoa, Cook Islands, Niue,
417 Samoa, Tokelau and Tuvalu (Fig.10 b). For PICTs located in the western side of the study region (Fiji, New
418 Caledonia, Solomon Islands, Tonga and Vanuatu), the maximum intensities are similar in hot and cold sea-
419 sons (Fig. 10 b). As shown also in section 3, for all PICTs, MHWs are much deeper in winter than in the hot
420 season, with 10% of the MHW events reaching depths more than > 200m around Fiji and Tonga.

421

422 Finally, the onset and decline rates are also shown. The faster the onset rate is, the quicker the MHW emerges,
423 and the shorter the reaction window for management responses is. The slower the decline rate is, the longer
424 it takes for the MHW to dissipate, and the slower heat is removed. Clearly, the onset rate is higher during the
425 hot season and lower in the cold season for all PICTs (Fig. 10 c, d). The median value is around 1.14 °C/day,
426 and 25% of all onset rates are >+ 0.3°C/day (Fig. 10 c), which is consistent with the results of Spillman et al.
427 (2021), but in the medium to high range compared to other regions (compare the values shown here with
428 Figure 3 from Spillman et al. (2021)). This is true for all PICTs, especially for Niue and Tokelau. In these
429 PICTs, where MHWs are typically short duration (Fig. 4 a), summer MHWs develop quickly, and marine
430 managers have little time to react. This also indicates rapid warming of the upper, shallow mixed layer (see
431 Fig. 6 e, f).

432

433 The pattern in the decline rate is similar to the onset rate. For all PICTs except Tuvalu, the decline rate is
434 larger in the hot season than in the cold season. This means that MHWs also dissipate more quickly in the
435 hot season, and prevent heat from stagnating.

436



437 Overall, we have found that Fiji, New Caledonia, Vanuatu and Tonga experience higher intensity and longer
438 lasting events, especially in the cold season, with deeper vertical extent. In the hot season, these countries
439 experience MHWs with higher intensities and longer durations, suggesting that these summer MHWs can be
440 particularly distressing for ecosystems there. They are among the most exposed countries in the region. The
441 Solomon Islands experience longer lasting events but these are generally of lower intensity.
442

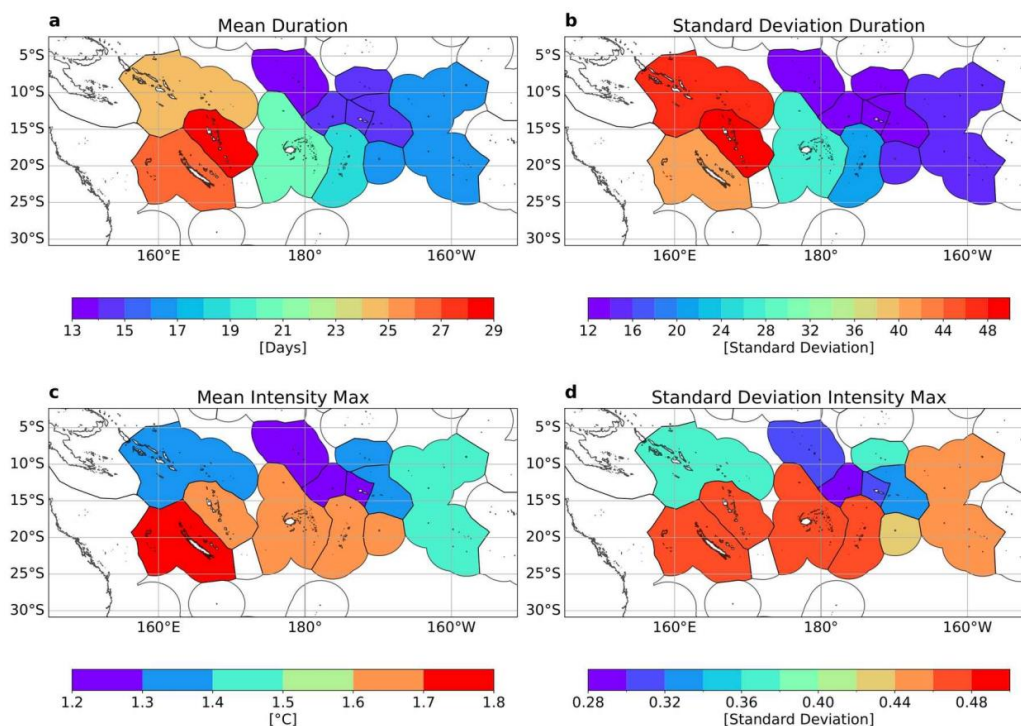


Figure 9 Mean and standard deviation of MHW duration a, b and mean intensity c, d, inside EEZs from Macroscale events. MHWs detected using NOAA-OISST from 1981-09 to 2023-06.

443

444



445

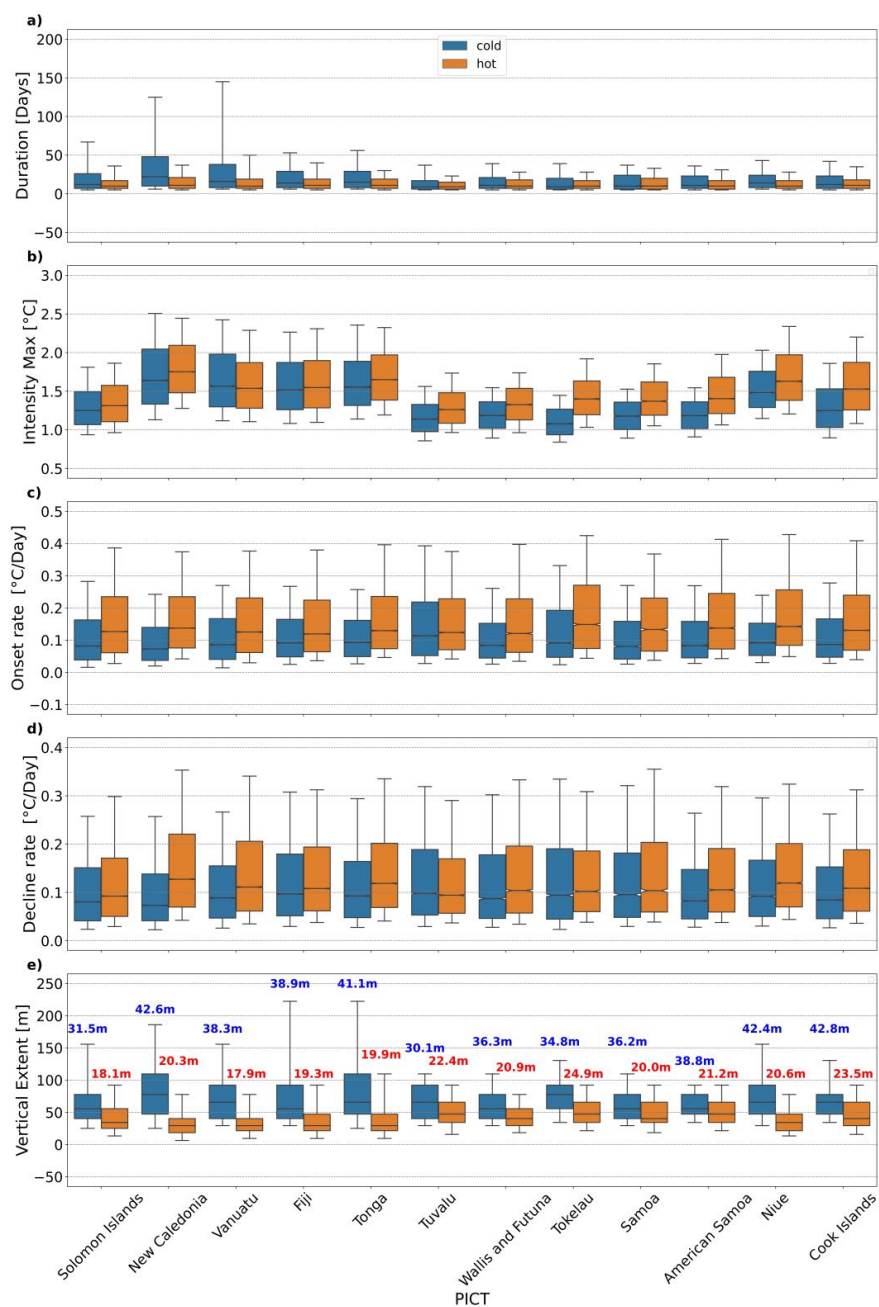


Figure 10 Box whisker plots showing MHW properties for macroscale events by Pacific Island Country and Territory (PICT) and seasons a, Duration, b, Mean Intensity, c, Onset rate, d, Decline rate and e, vertical extent. The red and blue texts in e are the mean mixed layer depth (MLD) in hot and cold season respectively. Lower edge of whisker marks 10th percentile, lower edge of box marks 25th percentile, the line in the middle marks the median, the upper edge of the box marks 75th percentile and the upper edge of the whisker marks 90th percentile. MHWs detected using NOAA-OISST from 1981-09 to 2023-06. MHW Vertical extents and mean Mixed Layer Depth obtained from GLORYS12 for period 1993 to 2019.



446 Figure 11 also shows the time series of the percentage fraction of EEZ in a MHW state, for two examples,
 447 New Caledonia and Fiji. This figure allows the identification of the main events that have impacted a large
 448 portion of the territory of each PICT, in both seasons. Some events – for example between 1997–1999,
 449 2010/11, 2015/16, 2020, and 2022, – covered more than 80% of the New Caledonia EEZ (Fig. 11 a). In the
 450 hot season, the largest events occurred in 1993, 2002, 2004, 2009, 2015, 2016 and 2022. These events, how-
 451 ever, were short lived. In Fiji, the events of 2010, hot season events from 2014 to 2017, and the events of
 452 2022, were most striking (Fig. 11 c).

453

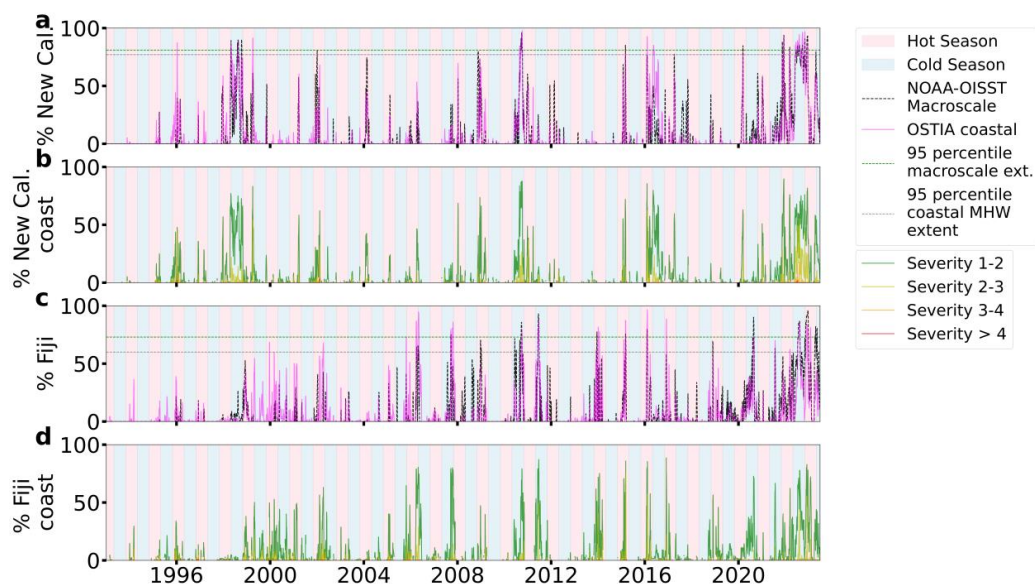


Figure 11 a,c, Time Series of % EEZ (in black dashed line) and % coastline (in magenta dashed line) in MHW state for New Caledonia and Fiji respectively. The horizontal green and gray dashed lines mark the 95 percentile of % EEZ covered by macroscale events and the 95 percentile of the % coastline in MHW state, respectively. b, d, Time Series of % coastline with 4 levels of severity for New Caledonia and Fiji respectively. Green line for severity 1 to 2, yellow for severity 2 to 3, orange for severity 3 to 4 and red for severity greater than 4. Coastal MHW and severity detected using OSTIA from 1993 to 2023, macroscale MHWs detected using NOAA-OISST from 1993 to 2023. In all panels a - d, the alternating pink and blue background colours represent the hot and cold season respectively.

454



455 **4.2 Coastal events: spatial structures**

456 We now investigate past MHW events around each country close to the coast, to provide answers to the
457 following questions: (1) are open ocean events observed at the coastal level too? (2) Which coastal areas
458 have been more impacted in the last decades? (3) Are there any refugia areas, less impacted by MHWs? (4)
459 Are coastal MHWs longer now or of stronger intensity compared with the past, and if so, where?

460

461 To answer questions (2) and (3), Fig. 12 and 13 show MHW properties around the coast of New Caledonia
462 and the Fijian archipelago, as examples, for both the cold and hot seasons using the OSTIA product, which
463 better resolves at the coastal scale. The same plots showing MHW properties at the coast, but using GLO-
464 RYS12, are also shown to estimate the robustness of the signals, and evaluate the ability of the GLORYS12
465 reanalysis to detect MHW near the coast. Coastal MHWs for Solomon Islands, Vanuatu and Tonga are shown
466 in Supplementary Figs. S1–S3. As shown in section 3, the small-scale MHWs events detected can be quite
467 different depending on the product, especially in the cold season. Here, only the robust patterns shown in
468 both products (OSTIA and GLORYS12) will be discussed.

469

470 As expected, the absolute number of MHW days at the coast are different among the two products, with
471 OSTIA indicating between 12 and 17 days every season, and GLORYS12 indicating between 15 and 25 days
472 of MHWs each season around New Caledonia's reef (Fig. 12 a,g compared to d,j). In both products, signifi-
473 cant contrasts between the various islands exist. The eastern coast of New Caledonia's main island, Grande
474 Terre, experiences generally longer but less intense MHWs than the western coast, both in the hot and cold
475 seasons. MHWs there are longer in the cold season, lasting > 25-30 days on average (Fig. 12 b,e,h,k). The
476 southwest coast of Grande Terre is exposed to short (< 15 days), but very intense (+2.5°C of maximum
477 intensity) MHWs in the hot season (Fig. 12 b,c,e,f). In these areas, southeasterly trade winds along the coast
478 favour occasional coastal upwelling events bringing colder waters to the surface, whose signature in SST is
479 modulated by the seasonal stratification (Alory et al., 2006; Marchesiello et al. (2010)). The MHW occur-
480 rence might be related to occasional cessation of upwelling explaining the short time scales of these events
481 and the high amplitude in a region with usually much colder (upwelling) conditions; this deserves more
482 investigation.

483

484 The northeastern part of the New Caledonian archipelago, equatorward of 19.5°S, comprising the north coast
485 of Grande Terre, the northern part of the Chesterfield Islands, and Entrecasteaux reefs, seem to be less exposed
486 to MHWs than the rest of New Caledonia, with less MHWs days, both in the cold and hot seasons, with small
487 maximum intensities (around +1.2-1.5°C). The southern part of the Chesterfields Islands is more exposed,
488 with more MHW days, of longer duration in the cold season, but of moderate intensity (+1.6°C in the hot
489 season, +1.4°C in the cold season).



490 Figure 13 presents MHW properties around coastal Fiji. Coastal Fiji experiences between 11 and 18 MHW
491 days per year, with certain parts of the Yasawas, parts of the Lau group and Kadavu having higher values in
492 the hot season compared to the cold season (Fig. 13 a,d). The opposite is true for GLORYS, where the number
493 of MHW days is generally higher in the cold season compared to the hot season. Generally, the mean MHW
494 duration around coastal Fiji is similar everywhere. In the hot season it is between 12 and 15 days and between
495 12 and 20 days in the cold season (Fig. 13 b,e,h,k). These values are much shorter than what is experienced
496 along coastal New Caledonia. The patterns in mean maximum intensity are quite similar between the hot and
497 cold seasons in coastal Fiji (between +0.8 to +1.6°C, Fig. 13, c,f,i,l), with the southern part of the country
498 experiencing more intense MHWs in both the hot and cold seasons.

499

500 To answer question (4), Fig. 14 shows locations with significant trends in annual number of MHW days
501 around coastal New Caledonia and Fiji for the OSTIA product. Similar trends are found with GLORYS12
502 (not shown). Significant trends in annual number of MHW days were observed around most of the coastlines
503 of the PICTs studied (Fiji, Fig. 14 b and Solomon Islands, Vanuatu and Tonga in Fig. S4; other PICTs not
504 shown). In New Caledonia, the only significant trends in MHWs days are found north of 20°S, especially
505 along the northeast coast of Grande Terre, which has significant positive trends of around 23 days of MHWs
506 per decade (Fig. 14 a), 1.5 times the typical number of current annual MHW days (approx. 14 MHW days
507 per year averaging over the seasons, Fig. 12 a,d). The trends in maximum intensity and other MHW param-
508 eters were not significant around most parts of New Caledonia (not shown). In Fiji, most of the coastline
509 shows a significant increasing trend of around 8 to 15 MHW days per decade (Fig. 14 b). However, the
510 southern coast of Viti Levu, all the way from coastal Suva to Lautoka and Rotuma, exhibits a stronger positive
511 trends in annual number of MHW days (between 18 and 20 days per decade) (Fig. 14 b), about 1.3 times the
512 typical number of MHW days per year (approx. 15 days per year from Fig. 13 a,d).

513

514 Are open ocean events observed at coastal level too? To answer this question (1), Fig. 11 shows the percent-
515 age of the coastline in MHW state for New Caledonia and Fiji, superimposed on the percentage of each EEZ
516 in MHW state. For the period between 1993 and 2023, most of the MHWs with large EEZ spatial coverage
517 were observed along large parts of the coastline as well (Fig. 11 a,c). In New Caledonia, 77% of days with
518 large macroscale events (greater than 80% of the EEZ, corresponding to the 95 percentile) also experienced
519 coastal events of large spatial extents (71% of the coastlines, corresponding to the 95 percentile). 53% of
520 MHW events that affected a large part of the coastlines, remained uniquely coastal, that is, not occurring
521 together with large macroscale events in the EEZ (Fig. 11 a). Coastal MHWs with large spatial extents are
522 more prevalent than large macroscale events in New Caledonia EEZ. A similar pattern was observed in Fiji.
523 Sixty eight percent of large macroscale events in Fiji EEZ coincided with a large part of the coastline being
524 in a MHW state as well, with 60% of large-scale coastal events (greater than 60% of the coastlines, corre-
525 sponding to the 95 percentile) being uniquely large coastal MHW days (Fig. 11 c). The events of 1997-1999,



526 2010/11 and 2022, affected large parts of the EEZ and the coastline in both New Caledonia and Fiji. While
527 the events seem to peak in the hot season, some large scale events extend across several seasons (including
528 the cold season), for example, the 1997-1999 and 2022 events in New Caledonia and the 2022 event in Fiji.
529 The severity of coastal MHW events are usually between 1 and 3 (Fig. 11 b,d) which corresponds to Moderate
530 to Strong events according to naming criteria established by Hobday et al. (2018). While it is known that
531 high severity index events in the hot season may have detrimental effects on coastal ecosystems, for example
532 fish kills in coastal Fiji in February 2016 noted in H22 (high percentage of high severity events in the 2016
533 hot season around Fiji, Fig. 11 d), it is uncertain if high severity index events in the cold season detrimentally
534 affected coastal ecosystems as no bleaching events were observed along coastal New Caledonia in the cold
535 season of 2022, despite the severity index being higher than usual around that time (Fig. 11 b).

536

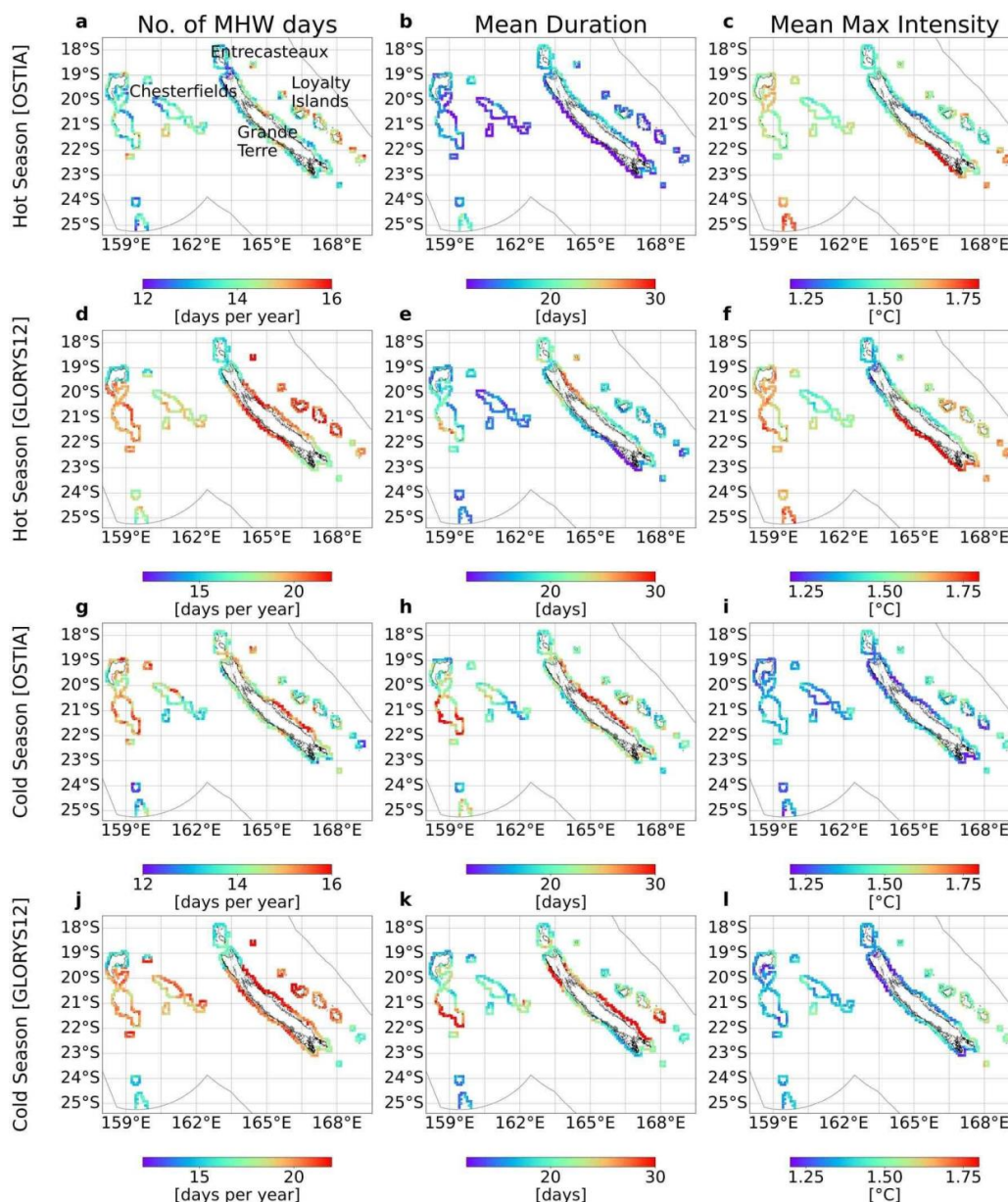


Figure 12 Total number of MHW days, mean Duration and mean Max Intensity in coastal New Caledonia , in hot season; a,b,c, in OSTIA , d,e,f, in GLORYS12, and in cold season g,h,i in OSTIA, j,k,l, in GLORYS12. MHWs detected using OSTIA and GLORYS12 from 1993-01 to 2023-10. The colorbar in a,g have been adjusted to reflect the spatial variability in the number of MHW days in OSTIA’s hot and cold season for New Caledonia coastline.

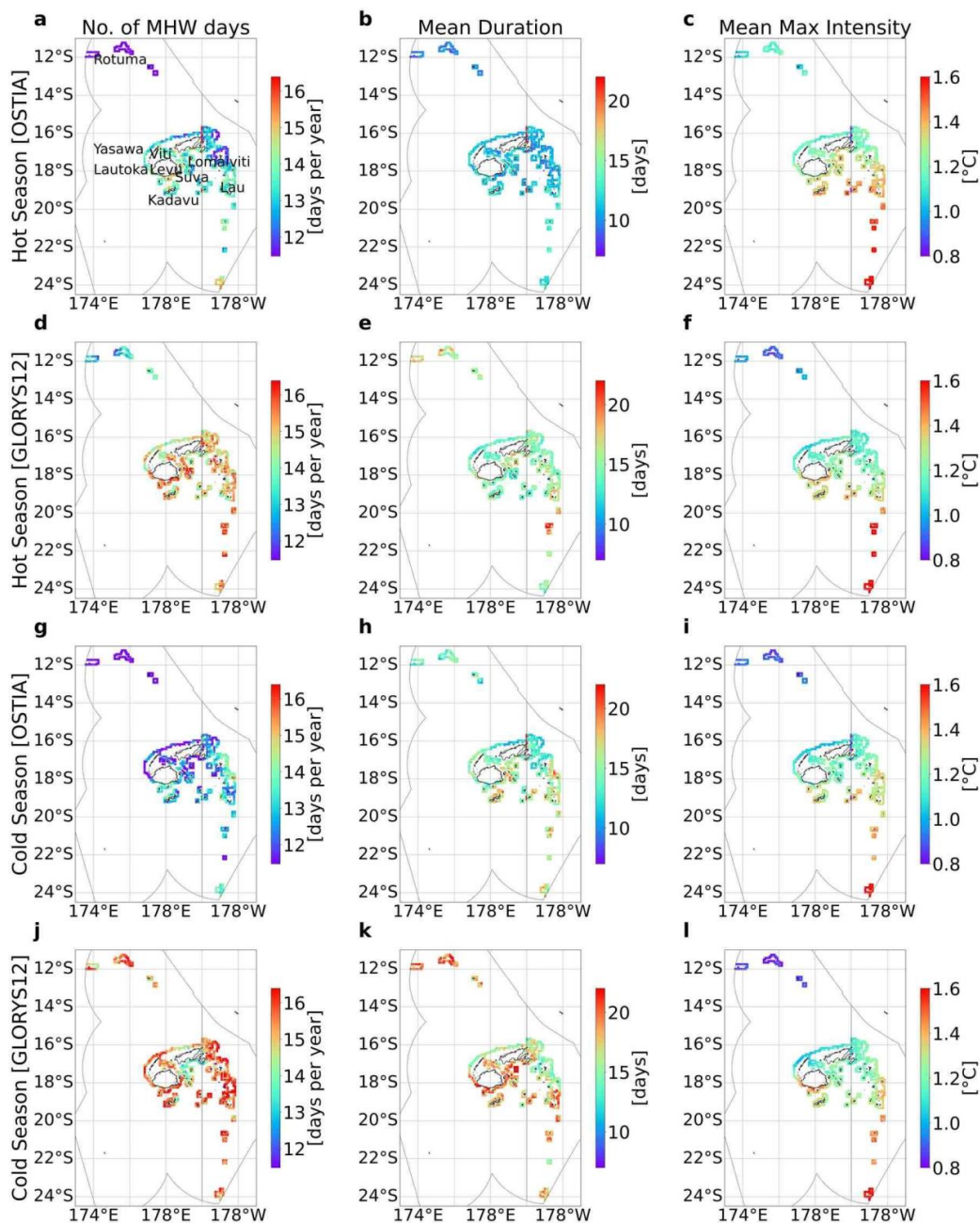


Figure 13 Total number of MHW days, mean Duration and mean Max Intensity in coastal Fiji , a, b, c, in OSTIA , d,e,f, in GLORYS12 in hot season and g,h,i in OSTIA, j,k,l, in GLORYS12 in cold season. MHWs detected using OSTIA and GLORYS12 from 1993-01 to 2023-10.

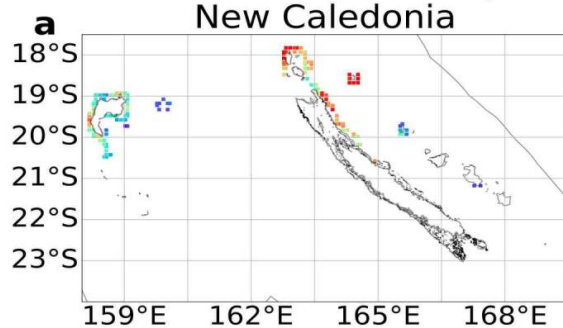


539

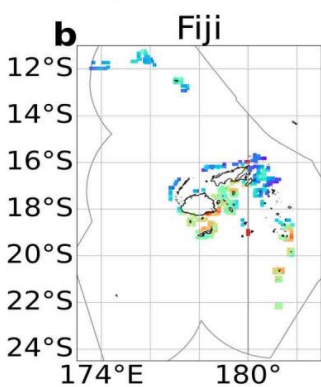
540

541

Total annual MHW days trend per decade New Caledonia



[days per decade]



[days per decade]

Figure 14 Significant trends in annual number of coastal MHW days in New Caledonia, a and coastal Fiji, b. MHWs detected using OSTIA from 1993 to 2022. The data in the maps refer to average changes in these metrics per decade over the 29 years.

542



543 **4.3 Coastal events: statistics for each country**

544

545 Figure 15 shows the seasonal distribution of coastal MHW properties (MHW duration, max intensity, onset
546 and decline rates) in the 12 PICTs studied in the form of box whisker plots for OSTIA. The duration of
547 MHWs can be much longer for coastal events compared to macroscale events. In the cold season, 75% of the
548 events have MHW durations of up to or longer than 80 days in New Caledonia, and Vanuatu (Fig. 15 a),
549 compared to up to 40 days during macroscale events (Fig. 10 a). The patterns and values in intensity are
550 similar for coastal and macroscale events for all the 12 PICTs. The median maximum intensities are typically
551 higher in the hot season for all countries except Fiji, New Caledonia, Solomon Islands, Tonga and Vanuatu,
552 where the difference between the seasons is small or there are higher maximum intensities in the cold season
553 (Fig. 15 b). This is an indication of some very high intensity events occurring in the cold season around the
554 coastlines of these six PICTs. The onset and decline rates are smaller in value for the coastal events (Fig. 15
555 c,d) compared to macroscale events (Fig. 10 c,d). This suggests that these PICTs could have a longer time to
556 prepare (that is, the reaction window is longer) for coastal MHWs compared to macroscale events. The slower
557 onset and decline rates in coastal MHWs could also be the reason why they have longer durations compared
558 to macroscale events.

559

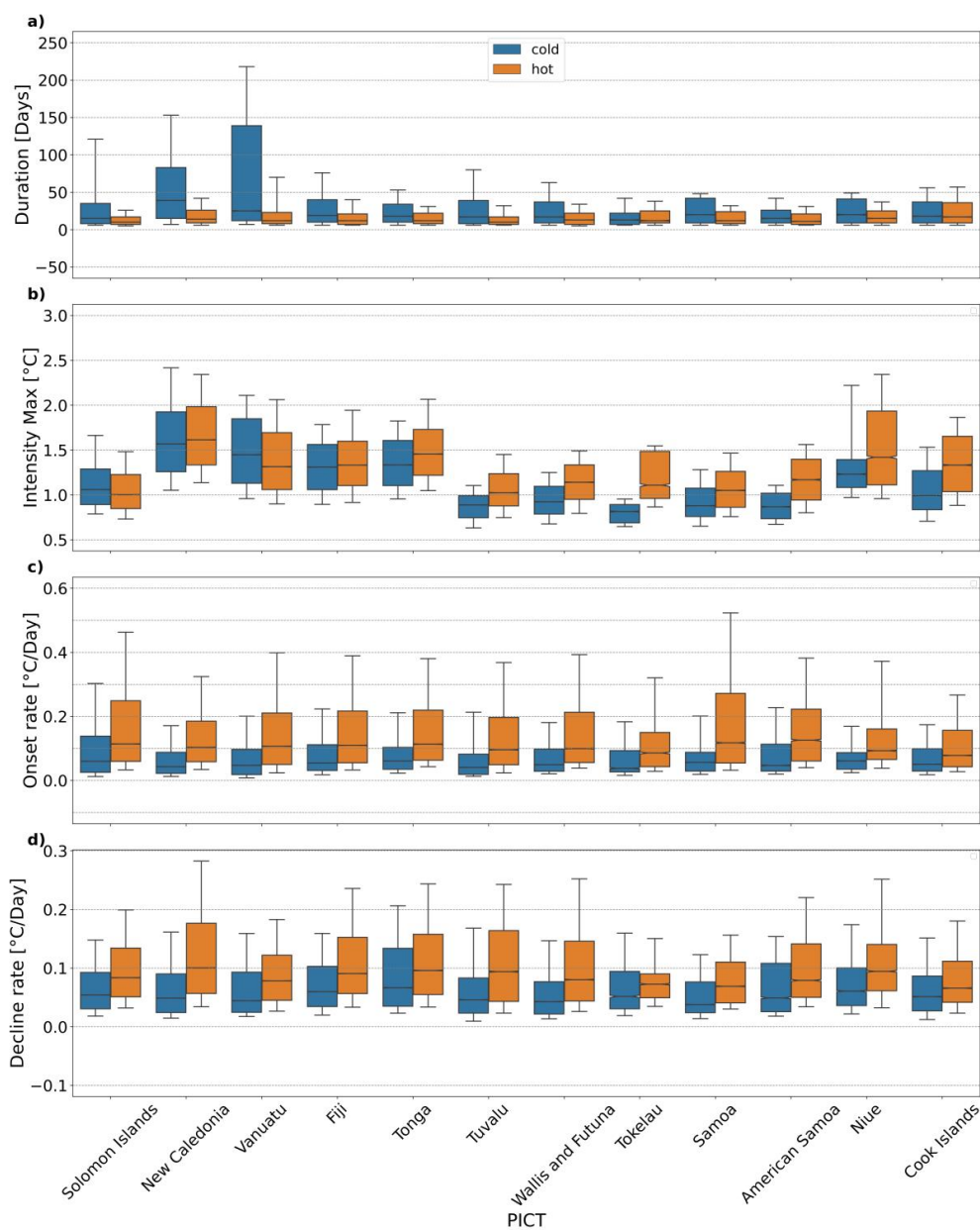


Figure 15 Box whisker plots showing MHW properties for coastal events by Pacific Island Country and Territory (PICT) and seasons a, Duration, b, Max Intensity, c, Onset rate and d, Decline rate. Lower edge of whisker marks 10th percentile, lower edge of box marks 25th percentile, the line in the middle marks the median, the upper edge of the box marks 75th percentile and the upper edge of the whisker marks 90th percentile. MHWs detected using OSTIA from 1993-01 to 2023-10.



561 **5 Discussion**

562 In this paper, we investigated the characteristics of past MHWs in the Southwest Pacific. One novelty of this
563 work is that we revisited the past MHWs statistics by distinguishing between macroscale and microscale
564 events, and among hot and cold seasons. We also described the statistics of past MHWs for each PICT. For
565 each EEZ, we provided information on their vertical extent and on their signatures at the coast. This provides
566 important elements that allow both (i) a better understanding of the physical processes that generate MHWs,
567 and (ii) a better anticipation of their impacts on ecosystems.

568

569 **5.1 What does this paper tell us about possible physical drivers?**

570 We showed that the characteristics of past MHWs (duration, intensity, and vertical extent) depend on their
571 size, and on the subregion considered. We now discuss what this can tell us in terms of the physical processes
572 driving the MHWs, and what governs these processes, for the five subregions identified. The spatial extent
573 of the MHW provides clues about its drivers: a large-scale event is likely driven by a large-scale climate
574 mode (e.g. Dutheil et al., 2024), while a small-scale event is more likely driven by a local advection or
575 atmospheric forcing process. While still in its infancy, the exploration of MHW vertical extent also provides
576 some interesting information on the MHW dynamics: shallow MHWs are more likely to be generated by
577 mixed layer depth dynamics, and deep MHWs by advection, or downwelling linked to planetary waves or
578 anticyclonic eddies. Recent work has led to the classification of the types of MHW events that can occur in
579 the vertical dimension (i.e. shallow, subsurface reversed/intensified, deep/extended events) (Schaeffer et al.,
580 2023; Zhang et al., 2023), characterisation based on surface features (e.g. block-like, deepening, shoaling,
581 multi-surfacing) (Köhn et al., 2024), as well as exploration of the mechanisms underpinning such events
582 (Elzahaby et al., 2021).

583

584 Previous studies investigating the physical processes and drivers generating MHWs have found ENSO to be
585 one of the important modulators of MHW activity (in terms of extent, duration and intensity) in this area (Sen
586 Gupta et al., 2020). While El Nino has been found to enhance MHW occurrence in the central Pacific region,
587 it tends to suppress MHW occurrence in the western Pacific in a chevron shaped region extending towards
588 the east (opposite is true during La Nina) (Holbrook et al., 2019).

589

590 Some of our results are consistent with this view, but many other processes can generate MHWs. In subregion
591 3, the “Equatorial central region”, our results indeed showed that the MHWs detected are deep, of large scale
592 and long duration, and occur during El Nino events. MHW characteristics there are consistent with the deep-
593 ening of the thermocline in the region during the development of El Nino events. On the contrary, in subre-
594 gion 1, in the “South-SPCZ region”, MHWs exhibit a diversity of characteristics. Some of the large-scale



595 and long duration MHW, mostly occurring in winter, are related to La Nina years (not shown). Yet, several
596 other MHWs in the area occurring in summer are of shorter duration, are shallow and can occur throughout
597 the years independently of the ENSO phase. One of the most extensive MHW ever recorded in the southwest
598 tropical Pacific region occurred in February 2016, during El Nino (Dutheil et al., 2024) where the El Nino
599 was expected to induce cooler temperatures on average. That MHW event has been explained by exception-
600 ally clear skies and light winds allowing strong surface heating in response linked to the combined effects of
601 an El Nino and an MJO event (Dutheil et al. 2024). More studies will be required to characterise the various
602 processes driving other MHW events, but our analyses suggest that mixed layer dynamics and large-scale
603 atmospheric forcing events are important factors.

604

605 On the contrary, in the subregion 4 (the “Southeastern Australia eddy region”) of high EKE, where it has
606 been shown that eddies are ubiquitous, most of MHWs detected are of small scale and short duration, and
607 extend very deep. As suggested by previous studies, MHWs in this subregion are often associated with
608 mesoscale eddies (Bian et al., 2023) and driven by advection (Zhang et al., 2023); surface heat flux driven
609 MHWs (shallow to ~20 m or so) are also observed (Li et al., 2020; Gregory et al., 2024). In addition to
610 mesoscale eddies, oceanic downwelling Rossby waves, and downwelling-favourable winds are also MHW
611 drivers near the Australian coast (Li et al., 2023; Misra et al., 2021; Schaeffer & Roughan, 2017).

612

613 Finally, in subregion 5, the “subtropical region”, MHWs properties are a mix between subregion 1 and sub-
614 region 4. In this area, the oceanic circulation is quite complex, with a zonally and vertically sheared current
615 system comprising the westward South Caledonian Jet in subsurface, the eastward Subtropical Counter Cur-
616 rent and EAC eastern extension. Mesoscale eddies are also ubiquitous (Keppler et al., 2018). It is probable
617 that MHWs are of mixed generation processes, with large-scale atmospheric forcing contributing to large-
618 scale, shallow events, and mesoscale eddies superimposed contributing to smaller scale events, with much
619 deeper extents, as also suggested by Bian et al. (2023). Investigating the oceanic heat budget to understand
620 the physical processes at play for the main MHWs events, in the different regions, will help to better under-
621 stand the various MHW types and will be done in a forthcoming study.

622

623 **5.2 What do our results on the different characteristics of MHW imply for ecosystem vulnerability?**

624 Distinguishing between macro and micro-scale MHWs events, and providing information on their vertical
625 extent, their seasonality and their signatures at the coast are also important outcomes from an ecosystem point
626 of view, both for open-ocean ecosystems and coastal ecosystems.

627



628 In the open ocean, highly mobile pelagic fishes like tunas are likely not affected in the same way by small-
629 scale and large-scale events covering a few, versus hundreds or thousands of square kilometres, respectively.
630 While tunas' mobility means that they can easily escape from the former, it is conceivable that such species
631 may sometimes be exposed to sub-optimal environmental conditions for extended periods during larger scale
632 events, necessitating long-range distributional shifts to more favourable areas (Bond et al. 2015; Walker et
633 al., 2020). Moreover, the consequences for affected individuals' physiology, feeding, growth and reproduc-
634 tive success as well as overall fishery productivity can be substantial (e.g. Mills et al. 2013), yet often remain
635 uncertain, and hence unaccounted for in fisheries management (Jacox et al. 2020).

636

637 The PICTs located in subregion 1 – Papua New Guinea, Solomon Islands, New Caledonia, Fiji and Vanuatu
638 – each supporting commercially-important tuna fisheries and dependent economies (Vidal et al., 2024), have
639 all been exposed to macroscale MHWs over the past 40 years, affecting a large portion of their EEZ in both
640 cold and hot seasons. In the other PICTs, MHWs are generally of smaller size, potentially limiting the local
641 impact of MHWs on pelagic species like tunas; however, the cumulative impact of increasing regional MHW
642 intensity, duration and time spent in MHW state on pelagic and coastal fisheries resources remains unknown.
643 Dutheil et al. (2024) have shown that the 2016 MHW near New Caledonia deeply impacted surface chloro-
644 phyll also and it is hence likely that during these events, all trophic levels will be impacted in addition to
645 oxygen and nutrients. Further research will have to investigate how these effects can combine to impact the
646 trophic web.

647

648 The vertical extent of MHWs is also important for predicting ecosystem vulnerability. The extension of warm
649 waters deeper is likely to affect both the fish species but also the fisheries. As an example, pelagic fishes like
650 bigeye tuna (*Thunnus obesus*), yellowfin tuna (*T. albacares*) and albacore tuna (*T. alalunga*) regularly move
651 vertically through the water column to track prey resources and/or meet oxygen demands (Briand et al. 2011;
652 Arrizabalaga et al. 2015; Nikolic et al. 2017). Data from tagging studies and fishery catch records both
653 demonstrate these species' propensity to dive to depths of several hundred metres (Williams et al. 2015;
654 Schaefer et al. 2011; Forget et al. 2015; Abascal et al. 2018; Scutt Phillips et al. 2019), thereby traversing
655 habitats likely to be severely affected by MHWs at-depth, such as those associated with the El Nino – South-
656 ern Oscillation (ENSO) (Lehodey et al., 2020). Our results show that in the hot season, the majority of mac-
657 roscale MHWs are shallower than 50m depth; 90% of them are shallower than 100m for all PICTs. One
658 exception concerns the central equatorial Pacific, where pelagic species may be more impacted. In winter,
659 MHWs can extend deeper, especially around Solomon Islands, New Caledonia, Vanuatu, Fiji and Tonga. For
660 these PICTs, which are exposed to large-scale events, potential impacts on pelagic species are more likely.
661 The modification of the species habitat in the vertical also impacts species vulnerability to fisheries as they
662 may, for example and depending on the species, be able to escape (or inversely) the fishing gears more easily



663 in an extended (or reduced) favourable habitat. These considerations of modified fishing pressure versus fish
664 responses to MHW will have to be considered when estimating the impacts of MHWs on commercial fish.

665

666 For coastal ecosystems, the important thing is to know which MHW have formed at the coast. Some MHWs
667 can indeed affect a large part of an EEZ, but without forming at the coast, and therefore without any signifi-
668 cant impact on reef ecosystems, coastal fisheries or coastal resource management. Here, we have provided
669 information on past MHWs for each PICTs coast to help establish a link between observed and reported
670 impacts on coastal ecosystems (such as coral bleaching and mass mortality events), and to identify key coastal
671 MHW characteristics. For these ecosystems, already close to the thermal tolerance threshold, summer MHWs
672 may be particularly threatening, yet the consequences of such events remain highly uncertain. A logical next
673 next step is to work more closely with ecologists and coastal managers to understand the impacts on, and to
674 define relevant MHW indices and thresholds for coastal ecosystems across the region. Such information
675 could theoretically inform a risk assessment framework for coastal ecosystems and guide country-led adap-
676 tation planning (e.g. Woods et al., 2022).

677

678 **5.3 Dependence of our results on the product and methodology**

679 In this paper, we used three different sea surface temperature products for the analyses (NOAA-OISST,
680 GLORYS12 and OSTIA). The choice of these three products was made either because they are widely used
681 (as NOAA-OISST), because they have a good spatial resolution at the coast (OSTIA) or because they provide
682 the subsurface structure and vertical extent (GLORYS). This choice has also been motivated by the fact that
683 these three products have a Near Real Time mode or are used in forecast mode (for GLORYS): as such, they
684 are used for warning systems for stakeholders and scientists. As shown by others (and illustrated in Appendix
685 1), the MHWs detection method is highly sensitive to the product used. One of our important results is that
686 this sensitivity on SST products lessens when considering macroscale events: the confidence in the results
687 obtained for macroscale is thus higher. On the contrary, for coastal events, the results greatly depend on the
688 product used (see also Marin et al. 2021). To reinforce confidence in the statistics obtained, a multi-ensemble
689 approach for MHW analysis would be needed (Marin et al. 2021).

690

691 We also examined the MHWs long-term trends in the southwest Pacific, and showed that all 12 PICTs expe-
692 rienced MHWs in the past 30 years and that these events are getting more frequent with greater spatial extents,
693 longer durations, but with lower intensity. Moreover, the percentage of surface area of the study region in a
694 MHW state exhibits a significant increasing trend (Fig. 8). Over the past decade, there has not been a single
695 day when at least part of the region was not exposed to a MHW.

696



697 These results are essential due to the choice of our fixed baseline (1993-2019), that is, the period of time we
698 used as a reference to compute the “normal” seasonal cycle. They are also due to the fact that we did not
699 remove any long-term trend in the temperature fields. As discussed by several others (see Amaya et al. 2023
700 for a comment), the choice of baseline matters, and can modify the results significantly. We chose the fixed
701 1993-2019 baseline because we think that in this past period, it is important to describe the ‘total heat expo-
702 sure’, considering both temporary extreme heat events and long-term trends. To characterise MHWs in a
703 future climate, both approaches (fixed baseline and shifting baseline) will be necessary. This will allow man-
704 agers to better anticipate the potential MHW impacts on species which will adapt quickly to a slow temper-
705 ature increase but will still be vulnerable to heat extremes, and those who are sensitive to absolute thresholds
706 (see Amaya et al., 2023).

707

708 **5.4 Responding to MHW threats**

709 Better knowledge of past MHW characteristics around each country allows us to relate past bleaching or
710 mass mortality events observed by the local populations to historical MHWs, or to other external disturb-
711 ances. It also helps to predict the types of MHWs that will occur in the future and their probability of occur-
712 rence. By revealing which coastal areas experienced more MHWs, in which season, our results inform the
713 countries on the relative vulnerability of certain areas and ecosystems (e.g. those more susceptible to coral
714 bleaching, mass mortality of sessile marine species or thermal stress on resident, site-attached fishes). For
715 the macroscale events, our data on MHW vertical extent, and the percentage of the EEZ affected by MHWs
716 can help to better assess MHWs impacts on mobile pelagic fishes.

717

718 When communities and stakeholders are prepared, the negative impacts of stressors can be lessened, or some-
719 times mitigated (Woods et al., 2022). Hobday et al. (2023) proposed a table of action, which can be used by
720 researchers, industry, managers, policy makers and governments, to respond to potential MHW arrival in
721 several stages. The first step to take before any action plan is to assess the risk, revisiting past MHW statistics
722 for regions of interest, and determining, in particular, the reaction window. This is exactly what we did here.
723 Our findings indicate that the rate of onset of MHWs in summer, for all countries, is in the upper range of
724 the values observed at the global scale: MHWs develop quickly, and the preparation window for countries is
725 rather short. This preparation window is longer for coastal events, and for winter MHWs. Marine managers
726 should be prepared for rapid responses based on warning bulletins, as MHWs develop and evolve.

727 The next steps will be to work closely with ecologists and anthropologists to identify the vulnerable species,
728 populations and ecosystems, and to define threshold limits and bio-cultural indicators to better assess the
729 risk. Through the work presented in this paper, and these next steps, we hope to help PICTs and their com-
730 munities to become prepared for the threats that MHWs will represent in the near future.

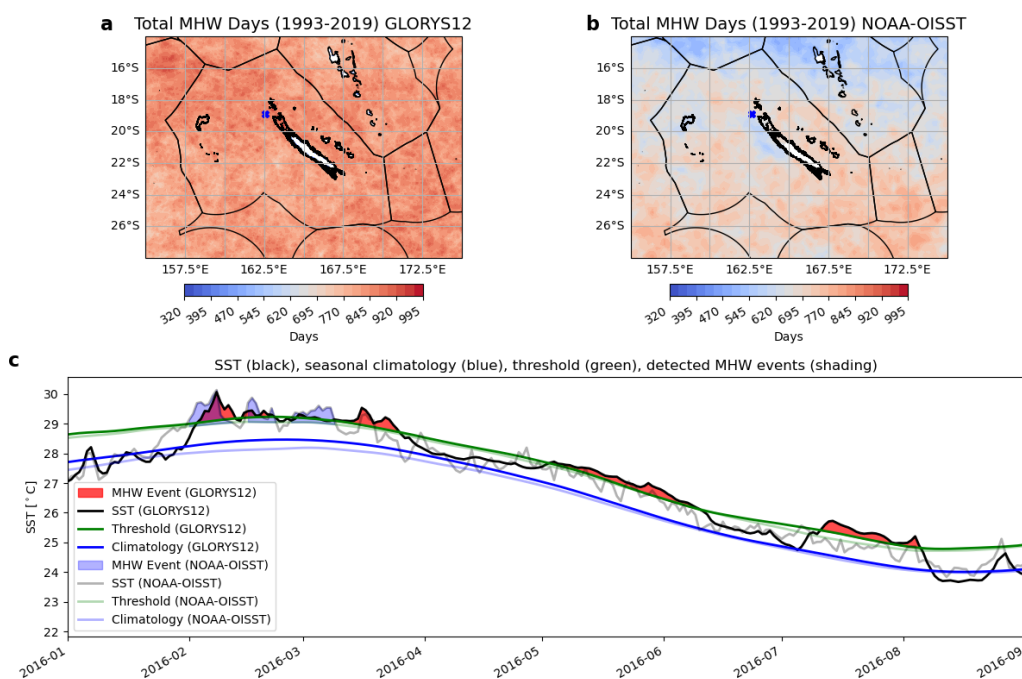


731 **Appendix A**

732 In this appendix, we illustrate how and why important differences may arise in MHW detection statistics
733 when applying the Hobday et al. (2016) detection method on two different, but similar, SST products. Figure
734 A1 (upper panels) shows the differences obtained in total MHW days between the two products, and Fig. A1
735 (lower) illustrates how such differences may arise during the year 2016. Even if the two climatologies and
736 90th quantile levels are close, GLORYS12 is a smoother SST product than NOAA-OISST, and the Hob16
737 method detects a greater number of longer duration MHWs events in GLORYS12, while it detects fewer
738 events and of shorter duration in NOAA-OISST.

739

740



741

742

743

744 **Figure A1: Upper panels: total number of MHWs days around New Caledonia for the period 1993-2019, detected**
745 **at each point with the method from Hobday et al. (2016) using two different SST products: GLORYS12 reanalysis**
746 **(upper left) and NOAA-OISST (upper right). Lower panel: Example of a timeseries at one particular location**
747 **Latitude = -18.89° Longitude = 162.58° for the 01/2016 to 09/2016 period for both products.**



748 **The darker colours and pink shading represent the MHW detected in GLORYS12 and the lighter colours and**
749 **blue shading is for MHWs detected in NOAA-OISST. The SST time series are shown in black and grey lines for**
750 **GLORYS12 and NOAA-OISST, respectively. The associated 1993-2019 climatologies are shown in blue (dark and**
751 **light), the 90th percentile threshold in green (dark and light).**

752

753

754

755

756

757

758

759

760

761

762



763 **Author Contributions**

764 SL, SC and CM led the design and implementation of the research, and wrote the first draft of the manuscript.
765 SL led the analyses and the preparation of the Figures. CD, JM, RL, IM, NH and SN contributed to text
766 sections. All authors contributed to manuscript revision, and read and approved the submitted version.
767

768 **Competing Interests**

769 The authors declare that they have no conflict of interest.
770

771 **Acknowledgments**

772 The authors gratefully acknowledge the contribution of Zijie Zhao of the University of Tasmania for his
773 assistance with spatial extent of MHWs and Awnesh Singh of the University of the South Pacific for his
774 support during the research. The authors would like to thank Eric Oliver for developing the Marine heatwaves
775 package and making it publicly available (<https://github.com/ecjoliver/marineHeatWaves>). The authors ap-
776 preciate organizations responsible for providing the data; NOAA-OISST from NOAA Physical Sciences La-
777 boratory, Boulder, Colorado, USA (<https://downloads.psl.noaa.gov/Datasets/noaa.oisst.v2.highres/>), GLO-
778 RYS-12 and OSTIA from Copernicus Marine Services and Mercator Ocean International (MOi)
779 (https://data.Marine.copernicus.eu/product/GLOBAL_MULTIYEAR_PHY_001_030/description),
780 [https://data.marine.copernicus.eu/product/SST_GLO_SST_L4_REP_OBSERVATIONS_010_011/ de-](https://data.marine.copernicus.eu/product/SST_GLO_SST_L4_REP_OBSERVATIONS_010_011/description)
781 [scription](https://data.marine.copernicus.eu/product/SST_GLO_SST_L4_REP_OBSERVATIONS_010_011/description)).
782

783 **Financial Support**

784 SL was funded by the Institut de Recherche pour le Développement (IRD) and the Pacific Community. SC,
785 CM and CD were funded by IRD. IM was funded by IRD and the New Caledonia Government (TICTAC
786 project). JM and SN were funded through the Pacific-European Union Marine Partnership (PEUMP) pro-
787 gram. NH acknowledges support from the ARC Centre of Excellence for Climate Extremes (CE170100023)
788 and Australia's National Environmental Science Program (NESP) Climate Systems Hub. The authors
789 acknowledge support from the Fonds Pacifique (HEAT project) and from the Agence Nationale de la Re-
790 cherche under the France 2030 program (MaHeWa project, ANR-23-POCE-0001).



791

792 **References**

793 Abascal, F. J., Peatman, T., Leroy, B., Nicol, S., Schaefer, K., Fuller, D. W., & Hampton, J. (2018). Spatio-
794 temporal variability in bigeye vertical distribution in the Pacific Ocean. *Fisheries Research*, 204, 371–379.

795 <https://doi.org/10.1016/j.fishres.2018.03.013>

796

797 Alory, G., Vega, A., Ganachaud, A., & Despinoy, M. (2006). Influence of upwelling, subsurface stratifica-
798 tion, and heat fluxes on coastal sea surface temperature off southwestern New Caledonia. *J. Geophys. Res.*
799 111. <https://doi.org/10.1029/2005JC003401>

800

801 Amaya, D., Jacox, M., Fewings, M., Saba, V., Stuecker, M., Rykaczewski, R., Ross, A., Stock, C., Capotondi,
802 A., Petrik, C., Bograd, S., Alexander, M., Cheng, W., Hermann, A., Kearney, K., & Powell, B. (2023). Marine
803 heatwaves need clear definitions so coastal communities can adapt. *Nature*, 616, 29–32.

804 <https://doi.org/10.1038/d41586-023-00924-2>

805

806 Arrizabalaga, H., Bruyn, P. de, Diaz, G. A., Murua, H., Chavance, P., Molina, A. D. de, Gaertner, D., Ariz,
807 J., Ruiz, J., & Kell, L. T. (2011). Productivity and susceptibility analysis for species caught in Atlantic tuna
808 fisheries. *Aquatic Living Resources*, 24(1), 1–12. <https://doi.org/10.1051/alr/2011007>

809

810 Bian, C., Jing, Z., Wang, H., Wu, L., Chen, Z., Gan, B., & Yang, H. (2023). Oceanic mesoscale eddies as
811 crucial drivers of global marine heatwaves. *Nature Communications*, 14(1), 2970.

812 <https://doi.org/10.1038/s41467-023-38811-z>

813

814 Bond, N. A., Cronin, M. F., Freeland, H., & Mantua, N. (2015). Causes and impacts of the 2014 warm
815 anomaly in the NE Pacific. *Geophysical Research Letters*, 42(9), 3414–3420.

816 <https://doi.org/10.1002/2015GL063306>

817

818 Bonino, G., Masina, S., Galimberti, G., & Moretti, M. (2023). Southern Europe and western Asian marine
819 heatwaves (SEWA-MHWs): A dataset based on macroevents. *Earth System Science Data*, 15(3), 1269–1285.

820 <https://doi.org/10.5194/essd-15-1269-2023>

821



- 822 Briand, K., Molony, B., & Lehodey, P. (2011). A study on the variability of albacore (*Thunnus alalunga*)
823 longline catch rates in the southwest Pacific Ocean. *Fisheries Oceanography*, 20(6), 517–529.
824 <https://doi.org/10.1111/j.1365-2419.2011.00599.x>
825
- 826 Brown, J. R., Lengaigne, M., Lintner, B. R., Widlansky, M. J., van der Wiel, K., Dutheil, C., Linsley, B. K.,
827 Matthews, A. J., & Renwick, J. (2020). South Pacific Convergence Zone dynamics, variability and impacts
828 in a changing climate. *Nature Reviews Earth & Environment*, 1(10), 530–543.
829 <https://doi.org/10.1038/s43017-020-0078-2>
830
- 831 Caputi, N., Kangas, M., Denham, A., Feng, M., Pearce, A., Hetzel, Y., & Chandrapavan, A. (2016). Man-
832 agement adaptation of invertebrate fisheries to an extreme marine heat wave event at a global warming hot
833 spot. *Ecology and Evolution*, 6(11), 3583–3593. <https://doi.org/10.1002/ece3.2137>
834
- 835 Cavole, L. M., Demko, A. M., Diner, R. E., Giddings, A., Koester, I., Pagniello, C. M. L. S., Paulsen, M.-L.,
836 Ramirez-Valdez, A., Schwenck, S. M., Yen, N. K., Zill, M. E., & Franks, P. J. S. (2016). Biological Impacts
837 of the 2013–2015 Warm-Water Anomaly in the Northeast Pacific: Winners, Losers, and the Future. *Ocean-*
838 *ography*, 29(2), 273–285.
839
- 840 Cravatte, S., Delcroix, T., Zhang, D., McPhaden, M., & Leloup, J. (2009). Observed freshening and warming
841 of the western Pacific Warm Pool. *Climate Dynamics*, 33(4), 565–589. [https://doi.org/10.1007/s00382-009-](https://doi.org/10.1007/s00382-009-0526-7)
842 [0526-7](https://doi.org/10.1007/s00382-009-0526-7)
843
- 844 Darmaraki, S., Somot, S., Sevault, F., & Nabat, P. (2019). Past Variability of Mediterranean Sea Marine
845 Heatwaves. *Geophysical Research Letters*, 46(16), 9813–9823. <https://doi.org/10.1029/2019GL082933>
846
- 847 Dixon, A. M., Forster, P. M., Heron, S. F., Stoner, A. M. K., & Beger, M. (2022). Future loss of local-scale
848 thermal refugia in coral reef ecosystems. *PLOS Climate*, 1(2), e0000004. [https://doi.org/10.1371/jour-](https://doi.org/10.1371/journal.pclm.0000004)
849 [nal.pclm.0000004](https://doi.org/10.1371/journal.pclm.0000004)
850
- 851 Dutheil, C., Lal, S., Lengaigne, M., Cravatte, S., Menkès, C., Receveur, A., Börgel, F., Gröger, M., Houl-
852 breque, F., Le Gendre, R., Mangolte, I., Peltier, A., & Meier, H. E. M. (2024). The massive 2016 marine
853 heatwave in the Southwest Pacific: An “El Niño–Madden-Julian Oscillation” compound event. *Science Ad-*
854 *vances*, 10(41), eadp2948. <https://doi.org/10.1126/sciadv.adp2948>
855



- 856 Elzahaby, Y., Schaeffer, A., Roughan, M., & Delaux, S. (2021). Oceanic Circulation Drives the Deepest and
857 Longest Marine Heatwaves in the East Australian Current System. *Geophysical Research Letters*, 48(17),
858 e2021GL094785. <https://doi.org/10.1029/2021GL094785>
859
- 860 Forget, F. G., Capello, M., Filmlalter, J. D., Govinden, R., Soria, M., Cowley, P. D., & Dagorn, L. (2015).
861 Behaviour and vulnerability of target and non-target species at drifting fish aggregating devices (FADs) in
862 the tropical tuna purse seine fishery determined by acoustic telemetry. *Canadian Journal of Fisheries and*
863 *Aquatic Sciences*, 72(9), 1398–1405. <https://doi.org/10.1139/cjfas-2014-0458>
864
- 865 Good, S., Fiedler, E., Mao, C., Martin, M. J., Maycock, A., Reid, R., Roberts-Jones, J., Searle, T., Waters,
866 J., While, J., & Worsfold, M. (2020). The Current Configuration of the OSTIA System for Operational Pro-
867 duction of Foundation Sea Surface Temperature and Ice Concentration Analyses. *Remote Sensing*, 12(4),
868 Article 4. <https://doi.org/10.3390/rs12040720>
869
- 870 Gregory, C. H., Holbrook, N. J., Spillman, C. M., & Marshall, A. G. (2024). Combined Role of the MJO and
871 ENSO in Shaping Extreme Warming Patterns and Coral Bleaching Risk in the Great Barrier Reef. *Geophys-*
872 *ical Research Letters*, 51(13), e2024GL108810. <https://doi.org/10.1029/2024GL108810>
873
- 874 Hobday, A. J., Alexander, L. V., Perkins, S. E., Smale, D., Straub, S., Oliver, E. C. J., Benthuyesen, J. A.,
875 Burrows, M. T., Donat, M. G., Feng, M., Holbrook, N. J., Moore, P. J., Scannell, H. A., Sen Gupta, A., &
876 Wernberg, T. (2016). A hierarchical approach to defining marine heatwaves. *Progress in Oceanography*, 141,
877 227–238. <https://doi.org/10.1016/j.poccean.2015.12.014>
878
- 879 Hobday, A. J., Burrows, M. T., Filbee-Dexter, K., Holbrook, N. J., Sen Gupta, A., Smale, D. A., Smith, K.
880 E., Thomsen, M. S., & Wernberg, T. (2023). With the arrival of El Niño, prepare for stronger marine heat-
881 waves. *Nature*, 621(7977), 38–41. <https://doi.org/10.1038/d41586-023-02730-2>
882
- 883 Hobday, A., Oliver, E., Sen Gupta, A., Benthuyesen, J., Burrows, M., Donat, M., Holbrook, N., Moore, P.,
884 Thomsen, M., Wernberg, T., & Smale, D. (2018). Categorizing and Naming Marine Heatwaves. *Oceanogra-*
885 *phy*, 31(2). <https://doi.org/10.5670/oceanog.2018.205>
886
- 887 Holbrook, N. J., Hernaman, V., Koshiba, S., Lako, J., Kajtar, J. B., Amosa, P., & Singh, A. (2022). Impacts
888 of marine heatwaves on tropical western and central Pacific Island nations and their communities. *Global*
889 *and Planetary Change*, 208, 103680. <https://doi.org/10.1016/j.gloplacha.2021.103680>



890

891 Holbrook, N. J., Scannell, H. A., Sen Gupta, A., Benthuisen, J. A., Feng, M., Oliver, E. C. J., Alexander, L.
892 V., Burrows, M. T., Donat, M. G., Hobday, A. J., Moore, P. J., Perkins-Kirkpatrick, S. E., Smale, D. A.,
893 Straub, S. C., & Wernberg, T. (2019). A global assessment of marine heatwaves and their drivers. *Nature*
894 *Communications*, 10, 2624. <https://doi.org/10.1038/s41467-019-10206-z>

895

896 Huang, B., Liu, C., Banzon, V., Freeman, E., Graham, G., Hankins, B., Smith, T., & Zhang, H.-M. (2021).
897 Improvements of the Daily Optimum Interpolation Sea Surface Temperature (DOISST) Version 2.1. *Journal*
898 *of Climate*, 34(8), 2923–2939. <https://doi.org/10.1175/JCLI-D-20-0166.1>

899

900 Hughes, T. P., Anderson, K. D., Connolly, S. R., Heron, S. F., Kerry, J. T., Lough, J. M., Baird, A. H., Baum,
901 J. K., Berumen, M. L., Bridge, T. C., Claar, D. C., Eakin, C. M., Gilmour, J. P., Graham, N. A. J., Harrison,
902 H., Hobbs, J.-P. A., Hoey, A. S., Hoogenboom, M., Lowe, R. J., ... Wilson, S. K. (2018). Spatial and temporal
903 patterns of mass bleaching of corals in the Anthropocene. *Science (New York, N.Y.)*, 359(6371), 80–83.
904 <https://doi.org/10.1126/science.aan8048>

905

906 IPCC. (2023). Summary for Policymakers. (Climate Change 2023: Synthesis Report. Contribution of Work-
907 ing Groups I, II and III to the Sixth Assessment Report of the Intergovernmental Panel on Climate Change,
908 pp. 1–34). IPCC. doi: 10.59327/IPCC/AR6-9789291691647.001

909

910 Jacox, M. G., Alexander, M. A., Bograd, S. J., & Scott, J. D. (2020). Thermal displacement by marine heat-
911 waves. *Nature*, 584(7819), Article 7819. <https://doi.org/10.1038/s41586-020-2534-z>

912

913 Jones, T., Parrish, J. K., Peterson, W. T., Bjorkstedt, E. P., Bond, N. A., Ballance, L. T., Bowes, V., Hipfner,
914 J. M., Burgess, H. K., Dolliver, J. E., Lindquist, K., Lindsey, J., Nevins, H. M., Robertson, R. R., Roletto, J.,
915 Wilson, L., Joyce, T., & Harvey, J. (2018). Massive Mortality of a Planktivorous Seabird in Response to a
916 Marine Heatwave. *Geophysical Research Letters*, 45(7), 3193–3202. <https://doi.org/10.1002/2017GL076164>

917

918 Keppler, L., Cravatte, S., Chaigneau, A., Pegliasco, C., Gourdeau, L., & Singh, A. (2018). Observed Char-
919 acteristics and Vertical Structure of Mesoscale Eddies in the Southwest Tropical Pacific. *Journal of Geo-*
920 *physical Research: Oceans*, 123(4), 2731–2756. <https://doi.org/10.1002/2017JC013712>

921

922 Köhn, E. E., Vogt, M., Münnich, M., & Gruber, N. (2024). On the Vertical Structure and Propagation of
923 Marine Heatwaves in the Eastern Pacific. *Journal of Geophysical Research: Oceans*, 129(1), e2023JC020063.
924 <https://doi.org/10.1029/2023JC020063>



925

926 Lehodey, P., Bertrand, A., Hobday, A. J., Kiyofuji, H., McClatchie, S., Menkès, C. E., Pilling, G., Polovina,
927 J., & Tommasi, D. (2020). ENSO Impact on Marine Fisheries and Ecosystems. In *El Niño Southern Oscilla-*
928 *tion in a Changing Climate* (pp. 429–451). American Geophysical Union (AGU).
929 <https://doi.org/10.1002/9781119548164.ch19>

930

931 Lellouche, J.-M., Greiner, E., Bourdallé-Badie, R., Garric, G., Melet, A., Drévilion, M., Clément, B., Hamon,
932 M., Le Galloudec, O., Regnier, C., Candela, T., Testut, C.-E., Florent, G., Giovanni, R., Mounir, B., Drillet,
933 Y., & Le Traon, P.-Y. (2021). The Copernicus Global 1/12° Oceanic and Sea Ice GLORYS12 Reanalysis.
934 *Frontiers in Earth Science*, 9. <https://doi.org/10.3389/feart.2021.698876>

935

936 Li, J., Roughan, M., & Hemming, M. (2023). Interactions between cold cyclonic eddies and a western bound-
937 ary current modulate marine heatwaves. *Communications Earth & Environment*, 4(1), 1–11.
938 <https://doi.org/10.1038/s43247-023-01041-8>

939

940 Marin, M., Feng, M., Phillips, H. E., & Bindoff, N. L. (2021). A Global, Multiproduct Analysis of Coastal
941 Marine Heatwaves: Distribution, Characteristics, and Long-Term Trends. *Journal of Geophysical Research:*
942 *Oceans*, 126(2), e2020JC016708. <https://doi.org/10.1029/2020JC016708>

943

944 Mills, K. E., Pershing, A. J., Brown, C. J., Chen, Y., Chiang, F.-S., Holland, D. S., Lehuta, S., Nye, J. A.,
945 Sun, J. C., Thomas, A. C., & Wahle, R. A. (2013). Fisheries Management in a Changing Climate: Lessons
946 from the 2012 Ocean Heat Wave in the Northwest Atlantic. *Oceanography*, 26(2), 191–195.

947

948 Misra, R., Sérazin, G., Meissner, K. J., & Sen Gupta, A. (2021). Projected Changes to Australian Marine
949 Heatwaves. *Geophysical Research Letters*, 48(7), e2020GL091323. <https://doi.org/10.1029/2020GL091323>

950

951 Moore, J. A. Y., Bellchambers, L. M., Depczynski, M. R., Evans, R. D., Evans, S. N., Field, S. N., Friedman,
952 K. J., Gilmour, J. P., Holmes, T. H., Middlebrook, R., Radford, B. T., Ridgway, T., Shedrawi, G., Taylor, H.,
953 Thomson, D. P., & Wilson, S. K. (2012). Unprecedented Mass Bleaching and Loss of Coral across 12° of
954 Latitude in Western Australia in 2010–11. *PLOS ONE*, 7(12), e51807. [https://doi.org/10.1371/jour-](https://doi.org/10.1371/journal.pone.0051807)
955 [nal.pone.0051807](https://doi.org/10.1371/journal.pone.0051807)

956

957 Nikolic, N., Morandau, G., Hoarau, L., West, W., Arrizabalaga, H., Hoyle, S., Nicol, S. J., Bourjea, J.,
958 Puech, A., Farley, J. H., Williams, A. J., & Fonteneau, A. (2017). Review of albacore tuna, *Thunnus alalunga*,



959 biology, fisheries and management. *Reviews in Fish Biology and Fisheries*, 27(4), 775–810.
960 <https://doi.org/10.1007/s11160-016-9453-y>
961
962 Oliver, E. C. J., Benthuisen, J. A., Darmaraki, S., Donat, M. G., Hobday, A. J., Holbrook, N. J., Schlegel, R.
963 W., & Sen Gupta, A. (2021). Marine Heatwaves. *Annual Review of Marine Science*, 13(1), 313–342.
964 <https://doi.org/10.1146/annurev-marine-032720-095144>
965
966 Phillips, J. S., Escalle, L., Pilling, G., Gupta, A. S., & Seville, E. van. (2019). Regional connectivity and
967 spatial densities of drifting fish aggregating devices, simulated from fishing events in the Western and Central
968 Pacific Ocean. *Environmental Research Communications*, 1(5), 055001. [https://doi.org/10.1088/2515-](https://doi.org/10.1088/2515-7620/ab21e9)
969 [7620/ab21e9](https://doi.org/10.1088/2515-7620/ab21e9)
970
971 Picaut J, Ioualalen M, Delcroix T, Masia F, Murtugudde R, Vialard J (2001) The oceanic zone of convergence
972 on the eastern edge of the Pacific warm pool: A synthesis of results and implications for El Niño-Southern
973 Oscillation and biogeochemical phenomena. *J Geophys Res Oceans* 106(C2):2363–2386. doi:10.1029/2000
974 JC900141
975
976 Plecha, S. M., & Soares, P. M. M. (2020). Global marine heatwave events using the new CMIP6 multi-model
977 ensemble: From shortcomings in present climate to future projections. *Environmental Research Letters*,
978 15(12), 124058. <https://doi.org/10.1088/1748-9326/abc847>
979
980 Qiu, B., Chen, S., & Kessler, W. S. (2009). Source of the 70-Day Mesoscale Eddy Variability in the Coral
981 Sea and the North Fiji Basin. *Journal of Physical Oceanography*, 39(2), 404–420.
982 <https://doi.org/10.1175/2008JPO3988.1>
983
984 Rocha, C. B., Gille, S. T., Chereskin, T. K., & Menemenlis, D. (2016). Seasonality of submesoscale dynamics
985 in the Kuroshio Extension. *Geophysical Research Letters*, 43(21), 11,304–11,311.
986 <https://doi.org/10.1002/2016GL071349>
987
988 Schaefer, K. M., Fuller, D. W., & Block, B. A. (2011). Movements, behavior, and habitat utilization of yel-
989 lowfin tuna (*Thunnus albacares*) in the Pacific Ocean off Baja California, Mexico, determined from archival
990 tag data analyses, including unscented Kalman filtering. *Fisheries Research*, 112(1), 22–37.
991 <https://doi.org/10.1016/j.fishres.2011.08.006>
992



- 993 Schaeffer, A., & Roughan, M. (2017). Subsurface intensification of marine heatwaves off southeastern Aus-
994 tralia: The role of stratification and local winds. *Geophysical Research Letters*, 44(10), 5025–5033.
995 <https://doi.org/10.1002/2017GL073714>
996
- 997 Schaeffer, A., Sen Gupta, A., & Roughan, M. (2023). Seasonal stratification and complex local dynamics
998 control the sub-surface structure of marine heatwaves in Eastern Australian coastal waters. *Communications*
999 *Earth & Environment*, 4(1), 1–12. <https://doi.org/10.1038/s43247-023-00966-4>
1000
- 1001 Sen Gupta, A., Thomsen, M., Benthuisen, J. A., Hobday, A. J., Oliver, E., Alexander, L. V., Burrows, M.
1002 T., Donat, M. G., Feng, M., Holbrook, N. J., Perkins-Kirkpatrick, S., Moore, P. J., Rodrigues, R. R., Scannell,
1003 H. A., Taschetto, A. S., Ummenhofer, C. C., Wernberg, T., & Smale, D. A. (2020). Drivers and impacts of
1004 the most extreme marine heatwave events. *Scientific Reports*, 10(1), Article 1.
1005 <https://doi.org/10.1038/s41598-020-75445-3>
1006
- 1007 Sérazin, G., Marin, F., Gourdeau, L., Cravatte, S., Morrow, R., & Dabat, M.-L. (2019). Scale-dependent
1008 analysis of in situ observations in the mesoscale to submesoscale range around New Caledonia.
1009 <https://doi.org/10.5194/os-2019-124>
1010
- 1011 Smith, K. E., Burrows, M. T., Hobday, A. J., Sen Gupta, A., Moore, P. J., Thomsen, M., Wernberg, T., &
1012 Smale, D. A. (2021). Socioeconomic impacts of marine heatwaves: Global issues and opportunities. *Science*,
1013 374(6566), eabj3593. <https://doi.org/10.1126/science.abj3593>
1014
- 1015 Spillman, C. M., Smith, G. A., Hobday, A. J., & Hartog, J. R. (2021). Onset and Decline Rates of Marine
1016 Heatwaves: Global Trends, Seasonal Forecasts and Marine Management. *Frontiers in Climate*, 3.
1017 <https://doi.org/10.3389/fclim.2021.801217>
1018
- 1019 Sun, D., Jing, Z., Li, F., & Wu, L. (2023). Characterizing global marine heatwaves under a spatio-temporal
1020 framework. *Progress in Oceanography*, 211, 102947. <https://doi.org/10.1016/j.pocean.2022.102947>
1021
- 1022 Thomson, J. A., Burkholder, D. A., Heithaus, M. R., Fourqurean, J. W., Fraser, M. W., Statton, J., &
1023 Kendrick, G. A. (2015). Extreme temperatures, foundation species, and abrupt ecosystem change: An exam-
1024 ple from an iconic seagrass ecosystem. *Global Change Biology*, 21(4), 1463–1474.
1025 <https://doi.org/10.1111/gcb.12694>
1026



- 1027 Uthicke, S., Logan, M., Liddy, M., Francis, D., Hardy, N., & Lamare, M. (2015). Climate change as an
1028 unexpected co-factor promoting coral eating seastar (*Acanthaster planci*) outbreaks. *Scientific Reports*, 5,
1029 8402. <https://doi.org/10.1038/srep08402>
1030
- 1031 van Hooidonk, R., Maynard, J. A., & Planes, S. (2013). Temporary refugia for coral reefs in a warming
1032 world. *Nature Climate Change*, 3(5), Article 5. <https://doi.org/10.1038/nclimate1829>
1033
- 1034 Vidal, T., Williams, P., & Ruaia, T. (2024, August 14). Overview of tuna fisheries in the Western and Central
1035 Pacific Ocean, including economic conditions – 2023—Rev.01 | WCPFC Meetings. [https://meet-](https://meetings.wcpfc.int/node/23098)
1036 [ings.wcpfc.int/node/23098](https://meetings.wcpfc.int/node/23098)
1037
- 1038 Vincent, E. M., Emanuel, K. A., Lengaigne, M., Vialard, J., & Madec, G. (2014). Influence of upper ocean
1039 stratification interannual variability on tropical cyclones. *Journal of Advances in Modeling Earth Systems*,
1040 6(3), 680–699. <https://doi.org/10.1002/2014MS000327>
1041
- 1042 Vogt, L., Burger, F. A., Griffies, S. M., & Frölicher, T. L. (2022). Local Drivers of Marine Heatwaves: A
1043 Global Analysis With an Earth System Model. *Frontiers in Climate*, 4.
1044 <https://doi.org/10.3389/fclim.2022.847995>
1045
- 1046 Walker, H. J., Hastings, P. A., Hyde, J. R., Lea, R. N., Snodgrass, O. E., & Bellquist, L. F. (2020). Unusual
1047 occurrences of fishes in the Southern California Current System during the warm water period of 2014–2018.
1048 *Estuarine, Coastal and Shelf Science*, 236, 106634. <https://doi.org/10.1016/j.ecss.2020.106634>
1049
- 1050 Wernberg, T., Smale, D. A., Tuya, F., Thomsen, M. S., Langlois, T. J., de Bettignies, T., Bennett, S., &
1051 Rousseaux, C. S. (2013). An extreme climatic event alters marine ecosystem structure in a global biodiversity
1052 hotspot. *Nature Climate Change*, 3(1), 78–82. <https://doi.org/10.1038/nclimate1627>
1053
- 1054 Woods, P. J., Macdonald, J. I., Bárðarson, H., Bonanomi, S., Boonstra, W. J., Cornell, G., Cripps, G., Dan-
1055 ielsen, R., Färber, L., Ferreira, A. S. A., Ferguson, K., Holma, M., Holt, R. E., Hunter, K. L., Kokkalis, A.,
1056 Langbehn, T. J., Ljungström, G., Nieminen, E., Nordström, M. C., ... Yletyinen, J. (2022). A review of
1057 adaptation options in fisheries management to support resilience and transition under socio-ecological
1058 change. *ICES Journal of Marine Science*, 79(2), 463–479. <https://doi.org/10.1093/icesjms/fsab146>
1059



1060 Wyatt, A. S. J., Leichter, J. J., Washburn, L., Kui, L., Edmunds, P. J., & Burgess, S. C. (2023). Hidden
1061 heatwaves and severe coral bleaching linked to mesoscale eddies and thermocline dynamics. Nature Com-
1062 munications, 14(1), Article 1. <https://doi.org/10.1038/s41467-022-35550-5>

1063

1064 Zhang, Y., Du, Y., Feng, M., & Hobday, A. J. (2023). Vertical structures of marine heatwaves. Nature Com-
1065 munications, 14(1), 6483. <https://doi.org/10.1038/s41467-023-42219-0>

1066

1067

1068